

**BALLISTIC IMPACT RESISTANCE OF GRAPHITE EPOXY COMPOSITES
WITH SHAPE MEMORY ALLOY AND EXTENDED CHAIN POLYETHYLENE
SPECTRA™ HYBRID COMPONENTS**

Roger L. Ellis

Thesis submitted to the Faculty of the Virginia Polytechnic Institute and State
University in partial fulfillment of the requirements for the degree of

Master of Science
in
Mechanical Engineering

Dr. Frederic Lalande, Co-Chairman
Dr. Craig A. Rogers, Co-Chairman
Dr. Victor Giurgiutiu

December, 1996
Blacksburg, Virginia

Keywords: Ballistic Impact, Hybrid Composites, Graphite Composites, SMA, Spectra™
Copyright 1996, Roger L. Ellis

BALLISTIC IMPACT RESISTANCE OF GRAPHITE EPOXY COMPOSITES WITH SHAPE MEMORY ALLOY AND EXTENDED CHAIN POLYETHYLENE SPECTRA™ HYBRID COMPONENTS

Roger L. Ellis

Abstract

Graphite epoxy composites lack effective mechanisms for absorbing local impact energy often resulting in penetration and a structural strength reduction. The effect of adding small amounts of two types of high strain hybrid components on the impact resistance of graphite epoxy composites subjected to projectiles traveling at ballistic velocities (greater than 900 ft/sec) has been studied. The hybrid components tested include superelastic shape memory alloy (SMA), a material having an unusually high strain to failure (15 - 20%), and a high performance extended chain polyethylene (ECPE) known as Spectra™, a polymer fiber traditionally used in soft and hard body armor applications.

A 1.2% volume fraction superelastic SMA fiber layer was embedded on the specimens front, middle, and backface to determine the best location for a hybrid component in the graphite composite. From visual observation and energy absorption values, it was concluded that the backface is the most suitable location for a high strain hybrid component. Unlike the front and middle locations, the hybrid component is not restricted from straining by surrounding graphite material. However, no significant increases in energy absorption were found when two perpendicular SMA layers and an SMA-aramid weave configuration were tested on the backface. In all cases, the embedded SMA fibers were pulled through the graphite without straining to their full potential. It is believed that this is due to high strain rate effects coupled with a strain mismatch between the tough SMA and the brittle epoxy resin. However, a significant increase in energy absorption was found by adding ECPE layers to the backface of the composite. With a 12% increase in total composite mass, a 99% increase in energy absorption was observed.

Acknowledgments

I would like to express my sincere thanks to all of the people who have assisted me in my efforts towards receiving a masters degree at Virginia Tech.

I am grateful to Dr. Craig Rogers, my advisor, in his support and for giving me the opportunity to perform this work. I wish to thank him for his confidence in me which was reflected in his flexibility, his willingness to let me decide the direction of this research, and to pursue it in a manner that I felt most suitable. I would also like to express my gratitude towards my co-advisor, Dr. Frederic Lalande. I appreciate the time he invested in advising me and for his openness, honesty, and sincerity.

I owe thanks to all of the people at the Center for Intelligent Material Systems and Structures who have always been willing to provide assistance, give advice, and be a friend. I would like to thank Victor Giurgiutiu, a member of my committee, for sharing his ideas and expressing interest in my research. Sincere thanks goes out to Beth Howell and Fanping Sun, who always assisted me with a smile. I am grateful for the friendships I have made with all of the graduate students and research scientists at CIMSS.

I wish to thank the engineers in the Armor Applications Development Group at Allied Signal Corporation for donating materials and allowing me to use their facilities to fabricate specimens. Their expert opinion and advice is greatly appreciated.

Thanks also goes out to Jeff Paine and Tom Kiesling for performing the work that led to this study.

I would also like to thank Bill Helbert who was an invaluable source of knowledge concerning ballistics and test methods. I appreciate his time and patience with our many tries at creating a suitable test facility.

Others that deserve thanks include the Virginia Tech Police Department for providing the 9mm handgun, the Army ROTC for allowing me to use their firing range, and the Textile Department for providing a weaving loom. Thanks also goes out to Danny Reed and the Center for Composite Materials for allowing me to use their facilities, and members of the Statistics Department for providing assistance.

I would like to sincerely acknowledge Dr. Gary Anderson and the Army Research Office for their financial support in this research (ARO-URI Grant No. DAAL03-92-G-0180)

I would not be truly thankful if I did not express gratitude towards my parents who raised me in an environment where I could realize and pursue my life's ambitions. Thanks also goes out to my grandfather who inspired me to be an engineer at a young age.

Above all, my deepest gratitude and love goes to my wife, Andrea. She is my inspiration and guiding light in everything I do. The many personal sacrifices Andrea has made for me to accomplish this work is greatly appreciated. She has been there through it all, the good and the bad. I will be eternally thankful for her understanding, support and love.

Contents

Chapter 1	1
Introduction	1
1.1 Motivation	1
1.2 Objective	1
Chapter 2	3
Literature Review	3
2.1 <i>Low Velocity Impact of Graphite Composites</i>	3
2.1.1 Low Velocity Damage Mechanisms	3
2.1.2 Low Velocity Impact Test Methods	4
2.1.2.1 Charpy and Izod Pendulum Impact Tests	4
2.1.2.2 Dropweight Impact Tests	5
2.1.2.3 Hydraulic Test Machines	5
2.2 <i>Improving Low Velocity Impact Damage Resistance</i>	5
2.3 <i>High Velocity and Ballistic Impact of Graphite Composites</i>	7
2.3.1 Localization Effect	8
2.3.2 Additional Damage Mechanism and the Penetration Process	8
2.3.3 Strain Rate Effects	10
2.3.4 Projectile Effects at High and Ballistic Velocities	10
2.3.5 Residual Strength vs. Resistance to Penetration	11
2.3.6 High and Ballistic Velocity Impact Test Methods	11
2.3.6.1 Projectile Acceleration Devices	12
2.3.6.2 Types of Projectiles	12
2.3.6.3 Method of Analysis	13
2.4 <i>Improving High and Ballistic Velocity Impact Damage Resistance</i>	14
Chapter 3	16
Experimental Procedure	16
3.1 <i>Objectives and Approach</i>	16
3.2 <i>Specimen Fabrication</i>	16
3.2.1 Control Specimens	16
3.2.2 SMA Hybrids	17
3.2.3 SMA-Kevlar Weave	18
3.2.4 Attaching ECPE Components	18
3.2.5 Embedding SMA in ECPE	19
3.3 <i>Test Method</i>	19
3.3.1 Military and NIJ Standards for Ballistic Impact Testing	19
3.3.2 Experimental Setup	20
3.3.3 Projectiles	22
3.3.4 Projectile Deployment	22

3.3.5 Test Procedure	22
3.3.6 Determination of the V_{50} Ballistic Limit	23
3.3.6.1 Determination of the Military V_{50} Ballistic Limit	23
3.3.6.2 Determination of the Logistic Regression V_{50} Ballistic Limit.....	23
3.3.7 Calculation of Energy Absorption Values.....	25
Chapter 4.....	26
Experimental Results	26
4.1 <i>Plain Graphite Specimens</i>	26
4.1.1 Impact Damage Mechanisms	26
4.1.2 Determination of the V_{50} Ballistic Limit for Plain Graphite Specimens	28
4.1.3 Projectile Effects	29
4.1.4 Effect of Four Shots Per Panel	30
4.2 <i>SMA Location Tests</i>	31
4.2.1 SMA Front Face Tests	31
4.2.2 SMA Middle Tests	32
4.2.3 SMA Back Face Tests	33
4.3 <i>SMA-Aramid Weave Tests</i>	34
4.4 <i>SMA Bi-directional Tests</i>	35
4.5 <i>Increased Volume Fractional Tests</i>	36
4.6 <i>ECPE Backface Tests</i>	36
4.7 <i>ECPE-SMA Backface Tests</i>	39
4.8 <i>Summary of V_{50} Ballistic Limit Results</i>	41
4.9 <i>Energy Absorption Comparisons</i>	41
Chapter 5	46
Conclusions	46
Chapter 6	48
Recommendations	48
References	50
Vita	58

List of Figures

Figure 2.1: Schematic demonstrating damage mechanisms for low velocity impact.....	3
Figure 2.2: Schematic of low velocity test methods; Charpy pendulum test and Izod pendulum test...4	
Figure 2.3: Stress strain curves of various materials.....	7
Figure 2.4: Representation of global deformation in low velocity impact (a) and local deformation in high velocity impact (b).....	8
Figure 2.5: Schematic representation of the shear plug damage mechanism.....	9
Figure 2.6: Schematic of delamination process in a cross-ply composite during high or ballistic velocity impact.....	9
Figure 2.7: Photo of fragment simulated projectiles.	12
Figure 3.1: Cure cycle for composite plates.....	17
Figure 3.2: Schematic demonstrating how SMA is embedded in graphite composite; a) Layup before consolidation b) Layup after consolidation.	17
Figure 3.3: Photo of weaving loom with SMA-Kevlar configuration.....	18
Figure 3.4: Cure cycle for ECPE prepreg.	19
Figure 3.5: Schematic of ballistic test setup following the NIJ standaed.....	20
Figure 3.6: Photo of gun in mount.....	21
Figure 3.7: Specimen frame mount with witness plate behind.....	21
Figure 3.8: Photo of projectile used for testing.....	22
Figure 3.9: Sketch of impact locations and firing order for specimen testing.....	22
Figure 3.10: Example demonstrating the general shape of a probability curve generated from logistic regression analysis of a data set.....	24
Figure 4.1: Graphite specimen impacted near its V_{50} ballistic limit shows a combination of shear plug, matrix cracking, delamination, and fiber failure.....	26

Figure 4.2: Photo of projectile and photo of specimen impacted near its V_{50} ballistic limit pointing out shear plug region. Note: Photos are at same scale.....27

Figure 4.3: Photo of a graphite specimen impacted near its V_{50} ballistic limit pointing out delaminations ends.28

Figure 4.4: Graphical representation of data points used to determine the military V_{50} ballistic limit for plain graphite composites.....28

Figure 4.5: Projectile deformations below first ply penetration level.....29

Figure 4.6: Various deformed projectiles after specimen penetration.30

Figure 4.7: C-scan of a graphite panel impacted in numbered order showing extent of delamination.30

Figure 4.8: Graphical representation of data points used to determine the military V_{50} ballistic limit for specimens with a 1.2 % volume fraction of uni-directional SMA fibers embedded on the front face of the composite.31

Figure 4.9: Additional damage in the composite is observed with SMA fibers embedded on front face (a) when compared to plain graphite (b).....32

Figure 4.10: Graphical representation of data points used to determine the military V_{50} ballistic limit for specimens with a 1.2 % volume fraction of uni-directional SMA fibers embedded in the middle of the composite.....32

Figure 4.11: Graphical representation of data points used to determine the military V_{50} ballistic limit for specimens with a 1.2 % volume fraction of uni-directional SMA fibers embedded on the backface of the composite.33

Figure 4.12: Graphical representation of data points used to determine the military V_{50} ballistic limit for specimens with a 1.2 % volume fraction of uni-directional SMA fibers with aramid weave embedded on the backface of the composite.....34

Figure 4.13: Photo of the backface of an impacted specimen containing a SMA-aramid weave hybrid component demonstrating single fiber shear pullout and poor interfacial bond.....35

Figure 4.14: Graphical representation of data points used to determine the military V_{50} ballistic limit for specimens with 2.4% volume fraction bi-directional SMA fibers embedded on the backface of the composite.....35

Figure 4.15: Photo of loops created by an SMA layer when impacted by a projectile.....36

Figure 4.16: Graphical representation of data points used to determine the military V_{50} ballistic limit for specimens with three ECPE prepreg layers bonded to the backface of the composite.....37

Figure 4.17: Graphical representation of data points used to determine the military V_{50} ballistic limit for specimens with six ECPE prepreg layers.37

Figure 4.18: Graphical representation of data points used to determine the military V_{50} ballistic limit for specimens with nine ECPE prepreg layers bonded to the backface of the composite.38

Figure 4.19: The post impact inspection of a specimen containing nine ECPE layers showed large deformation in the ECPE, which contributed to the significant improvement in energy absorption capabilities.38

Figure 4.20: Graphical representation of data points used to determine the military V_{50} ballistic limit for specimens with uni-directional SMA and three ECPE prepreg layers on the backface of the composite.39

Figure 4.21: Graphical representation of data points used to determine the military V_{50} ballistic limit for specimens with bi-directional SMA and three ECPE prepreg layers on the backface of the composite.40

Figure 4.22: Photo of the backface of an impacted ECPE-SMA uni-directional composite specimen demonstrating single fiber shear pullout.40

Figure 4.23: Photo of the backface of an impacted ECPE-SMA bi-directional composite specimen demonstrating the characteristic loop.41

Figure 4.24: Summary of the V_{50} ballistic limit values for each test configuration.42

Figure 4.25: Bar graph representing % increases in energy absorption when compared to plain graphite specimens.42

Figure 4.26: Bar graph representing % increases in mass and volume when compared to plain graphite specimens.43

Figure 4.27: Bar graph representing % increases in energy absorption normalized in weight and volume when compared to plain graphite specimens.44

Figure 4.28: Bar graph representing % increases in energy absorption per ounce of hybrid material.44

Figure 4.29: Bar graph representing % increases in energy absorption per in^3 of hybrid material.45

Figure 6.1: Drawing of suggested SMA weave pattern.48

List of Tables

Table 4.1: Results of a fifth shot in three of the plain graphite specimens.....	29
Table 4.2: Data from specimen containing 4.8% SMA volume fraction embedded on backface.	36

Chapter 1

Introduction

1.1 Motivation

Since their introduction, composite materials have been applied to a variety of structural applications. Among the most performant is the graphite or carbon fiber composite, which possesses one of the highest specific moduli. The specific strength and stiffness of graphite epoxy composites are significantly greater than monolithic materials such as steel and aluminum, which make them attractive for numerous weight critical applications.

Unfortunately, composites of this type have relatively poor mechanisms for absorbing energy due to local impact damage where loading is normal to the fiber plane. This is primarily due to the low strain to failure and low transverse shear strength of the graphite fiber and the brittle nature of the epoxy matrix. Since the early 1970's, researchers have been looking for methods to improve impact properties of graphite composites such as fiber and matrix toughening, interface toughening, through-the-thickness reinforcements, and hybridizing.

Impact events can be categorized into four velocity ranges; low, high, ballistic, and hypervelocity. Low velocity impact may include situations such as a dropped tool (< 100 ft/sec) whereas high velocity impact might include a bird colliding with an airplane (100 - 800 ft/sec). Ballistic impact events include situations such as a projectile fired from a gun at speeds in excess of 800 ft/sec. Finally, orbital debris traveling in outer-space at velocities up to 50,000 ft/sec are considered to be hypervelocity impact events (Schwinghamer, 1993; Schonberg and Yang, 1993).

The ballistic impact event is the focus of this Thesis. There is a growing need in military and civil applications for composite materials that not only have good structural characteristics, but also good penetration resistance and greater strength after impact. Composite parts in commercial and military aircraft are very susceptible to projectile impact such as bullets, fragments, or flying debris. If not contained, a projectile traveling at ballistic velocities could penetrate the composite and cause fires, hull damage, occupant injury, and malfunction of components within the aircraft. For example, the engine casing (nacelle) must be able to contain fragments traveling at ballistic velocities from a failed engine turbine rotor (Deluca, 1990). Also, an impact event may compromise the structural integrity of the composite and lead to failure. It is thus important for the composite material to maintain some structural integrity until the end of the mission or flight and prevent catastrophic failure. Other applications may also require both ballistic penetration resistance and structural integrity after impact; such as structural panels in lightweight armored cars and bomb containment.

1.2 Objective

The primary objective of this research is to investigate methods for improving the ballistic impact penetration resistance of graphite epoxy composites by including additional high-strain-energy hybrid components without significantly altering the base materials'

strength characteristics, weight, or volume. For this purpose, three hybrid components will be used: a nickel titanium alloy known as superelastic Shape Memory Alloy (SMA), an aramid known as Kevlar™, and a high performance extended chain polyethylene (ECPE) known as Spectra™.

This work is a continuation of previous studies (Kiesling, 1995; Paine, 1994) where the addition of small amounts of superelastic SMA fibers significantly improved the energy absorption capacity of graphite composites in quasi-static tests and low velocity impact tests resulting in complete penetration. In this thesis, the SMA's energy absorption capabilities when impacted at ballistic velocities will be determined.

Chapter 2

Literature Review

2.1 Low Velocity Impact of Graphite Composites

Considerable attention in the composite community has been given towards the effects of low velocity non-penetrating impact similar to that of a dropped tool, careless handling, or runway debris. This type of damage is most often undetectable by visual surface inspection (Choi and Chang, 1991), and can cause a significant reduction of the compression strength. In previous studies, it has been shown that low energy impacts may significantly reduce the load carrying capability of a composite component by as much as 50% (Cantwell et al., 1983; Cantwell et al., 1986; Dorey, 1984).

2.1.1 Low Velocity Damage Mechanisms

When traditional engineering materials such as steel and aluminum experience low velocity impact, the energy is typically absorbed through plastic deformation. Although this deformation is permanent, it usually does not significantly reduce the load carrying capability of the structure (Bradshaw et al., 1972).

Graphite composites however experience very little or no plastic deformation during low velocity impact because of the low strain to failure of the fiber and brittle nature of the epoxy matrix. Therefore, the impact energy is absorbed through various fracture processes. It has been well documented that the principal mechanisms for dissipating low velocity impact is through matrix cracking, delamination, and fiber failure (Lagace and Wolf, 1993; Choi and Chang, 1991; Cantwell and Morton, 1991; Cantwell and Morton, 1990a). Depending on the dimensions of the test specimens, such as in long thin beams, a portion of the impact energy can also be absorbed through global bending of the composite (Cantwell and Morton, 1990a). The three principal damage mechanisms are shown schematically in Figure 2.1.

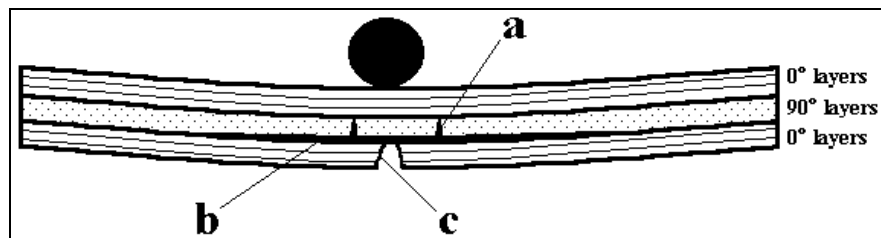


Figure 2.1: Schematic demonstrating the three principal damage mechanisms for low velocity impact: a) matrix cracking, b) delamination, c) fiber failure.

The extent of damage imposed by low velocity impact may be affected by the geometry and laminate configuration of the composite. Cantwell and Morton (1989a) found a top surface contact initial failure in short thick composites and a lower surface

flexural initial failure in long thin laminates. Based on a study by Choi et al. (1992), it was concluded that a change of stacking sequence has a more significant influence on the impact damage than a change of thickness.

2.1.2 Low Velocity Impact Test Methods

A wide variety of test methods for low velocity impact of composites have been used in the literature. Since most studies were for specific applications, it is often difficult to make adequate comparisons of results. The test methods most widely used include the Charpy pendulum, the Izod pendulum, the dropweight, and the hydraulic test machine.

2.1.2.1 Charpy and Izod Pendulum Impact Tests

The earliest methods used for low velocity impact testing were the Charpy pendulum (Novak and De Crescente, 1972) and the Izod pendulum (Chamis, et al., 1972). Both methods were originally designed for the testing of metallic materials. The Charpy test consists of a swinging pendulum impacting the center of a thick beam supported at both ends with a notch at the mid-plane, as shown in Figure 2.2(a).

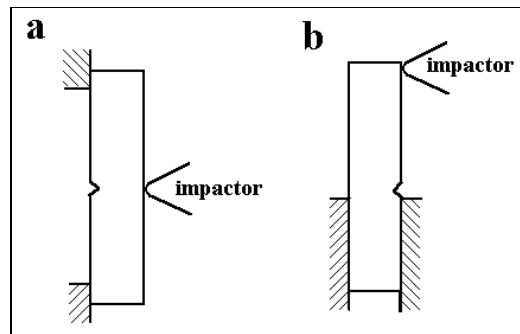


Figure 2.2: Schematic of low velocity test methods; a) Charpy pendulum and b) Izod pendulum.

The Izod test is similar to the Charpy test except that the notch is near the fixed end of the specimen while the impactor strikes the free end of the specimen as shown in Figure 2.2(b). The energy absorbed by the specimen is measured by the height of the swinging pendulum.

Although Charpy and Izod pendulum tests are easy to use, they have their disadvantages. The short and thick specimens used do not adequately represent typical engineering components. Beaumont et al. (1974) recognized significant deficiencies in the Charpy pendulum test in characterizing the response of materials. Therefore, an instrumented Charpy test that could differentiate between initiation and propagation energies was developed.

The Charpy and Izod tests can provide a simple method to gain insight to a materials performance. It has been suggested that these two tests are suitable for ranking the impact performance of various continuous fiber composites and as a first step in

determining the dynamic toughness of these materials (Cantwell and Morton, 1991; Chamis et al., 1972).

2.1.2.2 Dropweight Impact Tests

Another type of test used frequently is the drop weight impact test (Cantwell and Morton, 1989a,b,c, 1990a,b; Wang and Jang, 1991; Scott et al., 1991; Paine and Rogers, 1995). As its name suggests, an impactor of specific weight is dropped from a pre-determined height. One method for making energy calculations is by recording the rebound velocity of the impactor with optical sensors. Instrumented drop weight test machines that can measure the force versus time response make possible the study of the energy absorption through the different stages of specimen fracture. Also, the drop weight test allows for a greater variety of specimen geometry's, which is an advantage over the Charpy and Izod impact tests.

2.1.2.3 Hydraulic Test Machines

More recently, composite material properties have been studied with hydraulic test machines (Gillespie et al., 1987). Although an actual impact event does not occur, it can be simulated by testing the specimen at high strain rates. Extreme care must be taken when preparing the specimen and mounting it in the grips of the machine to prevent slippage at the clamped ends.

2.2 Improving Low Velocity Impact Damage Resistance

Since the early 1970's, researchers have been looking at various methods for improving the low velocity impact response of graphite composites. Oplinger and Slepetz (1975) concluded that "Any attempt to improve impact behavior must confront the low strain capability of graphite composites. Either graphite fibers with higher strain to fracture must be developed, or ways to reduce the local strain under the impacting object must be contrived." The methods of improving the damage resistance of graphite composites due to low velocity impact can be divided into five major areas; fiber toughening, matrix toughening, interface toughening, through-the-thickness reinforcements, and hybridizing.

Fiber toughening involves the use of graphite fibers developed with a higher strain to failure. The impact performance of this type of fiber has been evaluated with moderate success (Cantwell et al., 1986; Curtis 1984).

Several different approaches have been taken to toughen the matrix material. Although the stiffness of the composite is slightly reduced, one method of toughening the epoxy matrix is through the addition of rubber or thermoplastic compounds (Hedrick et al., 1993; Huang et al., 1993; Hunston et al., 1987; Williams and Rhodes, 1982). Scott et al. (1991) found an improvement in impact resistance without lowering the epoxy matrix modulus by the addition of fortifiers. Replacing epoxy with a high performance thermoplastic matrix with a stiffness comparable to epoxy material known as polyetheretherketone (PEEK) has also exhibited a higher resistance to impact (Wang and VuKhanh, 1991).

Since impact induced delamination occurs due to the graphite composites relatively low interlaminar strength, interface toughening through the use of adhesive layers has found success (Chan et al., 1986; Sun and Rechak, 1988; Bascom et al., 1993; Hoisington and Seferis, 1993). Because the additional adhesive layers may cause a great weight penalty, Rechak and Sun (1990) demonstrated how the placement of adhesive layers can be optimized to obtain the greatest benefit in improving impact resistance.

Another method for decreasing the amount of delamination caused by low velocity impact is through-the-thickness reinforcements such as braiding, three dimensional weaving, and stitching (Jang and Chung, 1986; Su, 1989; Kang and Lee, 1994). Although significant delamination reductions are achieved, these techniques are costly and degrade the in-plane properties due to fiber impalement. Advanced stitching techniques are being developed to reduce these disadvantages (Maiden and Ebersol, 1991).

Hybridizing graphite composites with additional tough high strain energy fibers have been shown to improve the damage tolerance due to low velocity impact (Jang et al., 1989; Wang and Jang, 1991). Fibers used in hybridizing include; S-Glass (Adams and Miller, 1975; Pavithran et al., 1991; Harris and Bunsell, 1975; Manders and Bader, 1981), aramid known as Kevlar™ (Dorey et al., 1978; Wardle, 1982; Marom et al., 1986), and extended chain polyethylene known as Spectra™ (Peijs and Venderbosch, 1991; Cordova and Bhatnager, 1987; Poursartip et al., 1987). The high strain capabilities of these fibers allow the impact energy to be spread over a wider area allowing the load to be shared by a greater volume of material. In most cases, however, the improved impact damage resistance is achieved at the expense of a reduction in the intended load bearing ability of the composite.

Of particular interest to this work is the hybridizing of graphite composites with a superelastic nickel titanium alloy known as Shape Memory Alloy (SMA). This metallic alloy has a high strain to failure exceeding 20% (Paine, 1994). The high strain capabilities of SMA fibers is primarily due to a stress induced martensitic phase transformation creating a plateau region in the stress strain curve, as shown in Figure 2.3. Also, the superelastic SMA has a significantly higher maximum strain energy value when compared to several various materials.

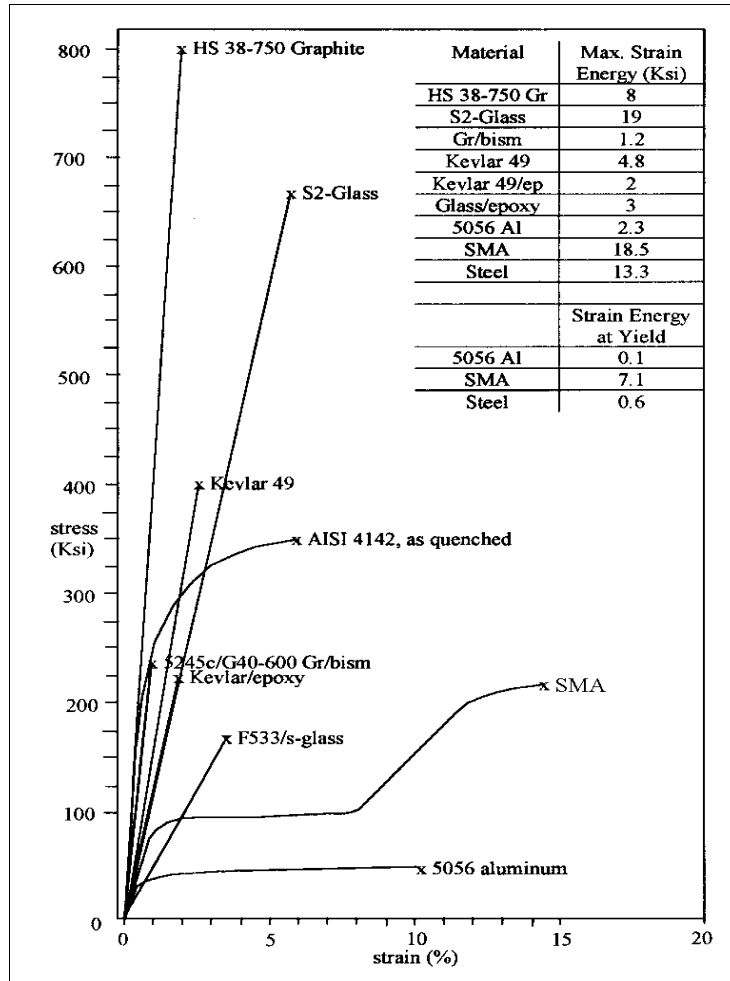


Figure 2.3: Stress strain curves of various materials (Kiesling, 1995).

It has been found that the addition of small amounts of superelastic SMA fibers to graphite composites can improve its low velocity impact damage resistance. Paine and Rogers (1994) found a 25% reduction in impact induced delamination with only a 2.8% volume fraction of embedded SMA. An increase in absorbed energy of 41% was found with a 6% volume fraction of embedded SMA (Kiesling 1996). A greater resistance to initial penetration, when compared to aluminum and Kevlar, was found with an SMA layer bonded layer bonded to the front face (Paine and Rogers, 1995).

2.3 High Velocity and Ballistic Impact of Graphite Composites

Although some of the high and ballistic velocity impact damage mechanisms are similar to those at low velocity, the response of a structural graphite composite is different and more complex. Furthermore, it is also more difficult to test at high and ballistic velocities. While most of the literature on the ballistic impact of composites are related to tougher, high strain materials such as aramids (Kevlar™), S-glass, and high performance

polyethylene (Spectra™), a few important studies have been performed on graphite composites (Cantwell and Morton, 1989a; Cantwell and Morton, 1989b; Cantwell and Morton, 1990a; Cantwell and Morton, 1990b; Hsieh et al., 1990; Jenq et al., 1992). An overview of the issues that makes the high and ballistic velocity impact different from low velocity impact will be presented.

2.3.1 Localization Effect

As discussed previously, some of the low velocity impact energy may be absorbed through global bending of the composite allowing energy transfer to locations away from the point of impact. Since the contact time between the projectile and the composite is considerably less at higher velocities, the impact loading induces a localized response with no global deformation. These two different types of impact, as suggested by Cantwell and Morton (1989b), are represented graphically in Figure 2.4. Cantwell and Morton (1989b) demonstrated this concept by looking at delaminations in beams of various lengths impacted at low and high velocities. It was found that the damage size decreased as the length of the beam increased when impacted at low velocities. At high velocities, however, the level of damage was independent of the length of the beam. It was also found that with a high specimen to mass ratio, the specimen boundary conditions have negligible effects on ballistic impact results. (Dikshit and Sundararajan, 1992).

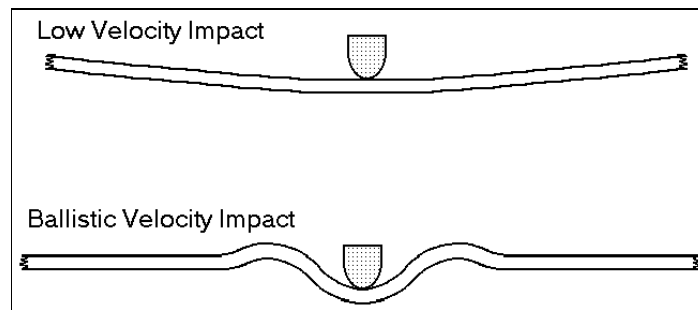


Figure 2.4: Representation of global deformation in low velocity impact (a) and local deformation in high velocity impact (b).

2.3.2 Additional Damage Mechanism and the Penetration Process

Since the high velocity impact energy is dissipated over a smaller region, an additional damage mechanism is present at higher velocities known as the shear plug. Due to the high stresses created at the point of impact, the material around the perimeter of the projectile is sheared and pushed forward causing a hole or “plug” slightly larger than the diameter of the projectile and increases as it penetrates the composite as shown in Figure 2.5.

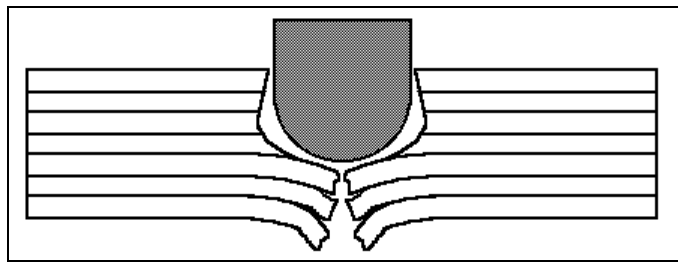


Figure 2.5: Schematic representation of the shear plug damage mechanism.

The entire high velocity projectile penetration process at higher velocities involves a combination of fiber shear (shear plug), matrix crack growth, delamination, and tensile fiber failure. The sequence of events for a cross-ply layup is described in great detail by Cristescu et al. (1975) which will be summarized here.

As discussed, upon impact of the first ply, the projectile energy is sufficient to cut the fibers in shear. This shear process continues in successive plies until the impact energy of the projectile is lowered to the point that the fibers can provide some resistance to shear. When this occurs, the fibers in contact with the projectile are pushed forward. This causes a line of matrix cracks within that ply to generate outward between fibers on either side of the projectile. This is demonstrated graphically in Figure 2.6 (top view) where ply (a) whose fibers are shown in the vertical direction are in front of ply (b) which contain fibers shown in the horizontal direction. The two solid vertical lines in the figure represents the matrix cracks formed. The fibers in contact with the projectile are pushed forward and the matrix cracking continues to grow in the vertical directions until all of the fibers in that strip are cut through. However, until the fibers are cut, the strip from lamina (a) loads transversely the second lamina (b) along the length of the line of matrix cracks and pushes it forward also. This causes a separation (delamination) between the unloaded fibers of ply (a) and the loaded fibers of (b). Once the fibers are all cut in ply (a) the process is repeated in ply (b). This delamination process continues as the projectile makes its way through the composite. Since it takes longer to penetrate each successive

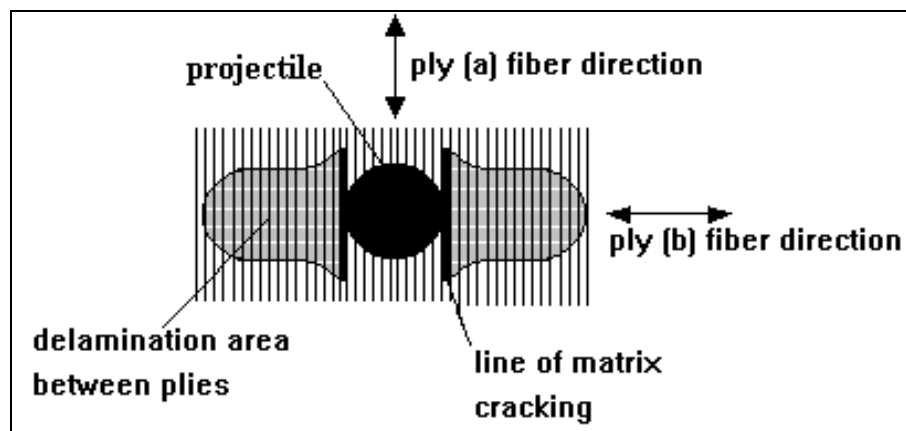


Figure 2.6: Schematic of delamination process in a cross-ply composite during high or ballistic velocity impact.

lamina, the separation between plies has more time to propagate outward causing the delamination area and extent of matrix cracking to grow as the projectile makes its way through the composite. This is continued until the projectile is either stopped or exits the composite.

2.3.3 Strain Rate Effects

For a .25” thick composite panel that stops a projectile traveling at 1000 ft/sec, the whole impact event occurs in 21 micro-seconds. With this short of an impact time, the strain rate effects must be considered. Much attention has been given to tough materials such as S-glass, aramids, and high performance polyethylene which behave differently at higher strain rates (Hsieh et al., 1990; Cuniff, 1992; Sloan and Nguyen, 1995). However, since graphite composites are inherently brittle during low, high, and ballistic velocity impact, strain rate effects are negligible (Hsieh et al., 1990).

2.3.4 Projectile Effects at High and Ballistic Velocities

At high and ballistic velocities, the action and characteristics of the penetrator have significant effects on test results. New issues that arise when testing at higher velocity schemes include; the shape and mass of the penetrator, the projectile deformation, and the spinning effects.

Although the shape of the penetrator can affect the degree of damage at all velocity ranges, the shape effect is greater at higher velocities. A sharp pointed projectile is going to penetrate further into a composite than a more blunt projectile of larger diameter but equal mass. The blunt projectile, however, may cause significantly more damage to the composite whereas the pointed projectile may just pierce entirely through leaving only a small hole. Jenq et al. (1992) found that the momentum transfer to graphite/epoxy targets by blunt impactors is about four times greater than that of a tip-ended penetrator when the penetrator is fired at ballistic velocities.

The effect of varying the mass of the projectile while maintaining the same size and shape has been studied by Cantwell and Morton (1989c). It was found that varying the mass of the projectile had a significant effect on the resulting damage to the composite. Cantwell and Morton (1989c) suggest that lighter projectiles are more damaging to the overall load-bearing capability of the composite because the incident energy is dissipated over a very small area immediately adjacent to the point of impact.

Another aspect of ballistic velocity testing is the projectile deformation that occurs at higher energy levels. Especially on composites with a hard front surface, pointed projectiles may become blunted upon impact. Savrun et al. (1991) found that the blunting a steel impacting projectile appeared to be the major defeat mechanism of a ceramic/Spectra™ hybrid. When performing ballistic testing with projectiles commonly used in civilian handguns and rifles, the projectile can easily deform since it is typically made of lead with a copper outer coating (jacket).

Finally, for ballistic testing, most projectiles are fired from some type of test barrel. For stability reasons, the barrel is designed so that the projectile is spinning as it leaves the device. This causes a type of drilling action as the projectile impacts the specimen. Also, if the test barrel is close to the specimen, the projectile may not have time to stabilize causing its tip to penetrate at an angle.

2.3.5 Residual Strength vs. Resistance to Penetration

Composite design becomes more application specific for protection against high and ballistic velocity impact of graphite composites. An approach towards design will depend greatly on the nature and dynamics of the projectile to be defeated as well as the desired end result. The attributes of the composite may be quite different if one is designing for greater strength after impact as opposed to designing for resistance to penetration. If one is designing for both, an optimal compromise between the two designs must be reached.

A few high and ballistic velocity impact studies have been performed to characterize the structural strength after impact (also known as residual strength) of graphite epoxy composites (Husman et al., 1975; Cantwell and Morton, 1990b; Jenq, Wang and Sheu, 1992; Suarez and Whiteside, 1975). It has been found that for a given impactor type, the level of damage increases with increasing impact energy up to the penetration velocity (also known as the ballistic limit), at which point the projectile barely perforates the target (Cantwell and Morton, 1989c). It can be concluded that as the level of damage increases, the structural strength of the composite after impact also decreases. However, at increasing impact energy levels greater than the penetration velocity, the level of damage decreases. It has been found that at velocities much greater than the perforation velocity, the hole in the material inflicted by the projectile produces the same reduction in residual strength as a hole with the same diameter that is cut or drilled out of the same material (Husman et al., 1975). Therefore, when designing for greater strength after impact where projectile containment is not of a concern, a material formulated with the least resistance to penetration while maintaining the structural strength requirements would be desired. If projectile containment is required then a substantial factor of safety must be used in the design. With graphite epoxy composites this usually means making the thickness significantly greater than that required by the structural load requirements.

Some design applications may require resistance to penetration but not require strength after impact. An example would be a lightweight armor car made of several smaller composite elements that must meet certain structural load characteristics while, at the same time, not allow a projectile to enter its interior. However, if a particular element becomes damaged, it could be easily replaced. This being the case, one would design the composite just below its penetration velocity to maximize the amount of energy that could be transferred to the composite, which will also maximize damage.

2.3.6 High and Ballistic Velocity Impact Test Methods

Several different approaches have been taken for testing and evaluating materials impacted at high and ballistic velocities. Various aspects of ballistic testing including projectile acceleration devices, types of projectiles used, and methods of analysis are presented.

2.3.6.1 Projectile Acceleration Devices

In order to achieve speeds above 1000 ft/sec, a projectile is propelled through a device (gun) having a cylinder (barrel) slightly larger than its diameter. A compressed gas or a burning powder has been used as propellants.

Projectiles fired from a gas gun is accomplished by pressurizing a chamber containing a plastic diaphragm restricting gas flow (usually nitrogen) into the barrel. When a predetermined pressure is reached, the diaphragm is burst by electrical heating and the projectile is accelerated. Gas guns are generally used for high velocity testing at typical speeds ranging from 200 ft/sec to 800 ft/sec. However, velocities as high as 2000 ft/sec have been achieved with more sophisticated systems (Cantwell and Morton, 1989c).

Ballistic velocities of 1000 ft/sec or more is usually accomplished through use of a burning powder gun. The projectile is propelled using a powder that is explosive upon ignition. Velocity is controlled by using a pre-determined amount of charge. Extreme velocities as high as 9000 ft/sec can be obtained (Husman et al., 1975).

2.3.6.2 Types of Projectiles

As discussed previously, the characteristic of the projectile used may have significant effects on impact results. Projectiles used for high and ballistic velocity testing include machined steel cylinders and spheres, fragment simulated projectiles, and commercial ammunition.

Machined steel cylinders and spheres are often used for gas gun testing (Cantwell and Morton, 1989b,c, 1990a,b; Cristescu et al., 1975; Jenq et al., 1992). They are used because they can be easily purchased or fabricated in a machine shop to fit the dimensions of the test barrel. Projectiles of this type are also good for comparison since typical low velocity impactors are similar in nature. Projectile deformation is minimal, thus avoiding an additional test variable. The disadvantage of a machined steel projectile is that it may not adequately represent foreign threats one might be designing for.

As its name suggests, the fragment simulated projectile (FSP) was developed by the U.S. Army in order to simulate metal fragments encountered in war. FSP's, which are manufactured according to military specification MIL-P-46593A, are cylindrical with a blunt chisel shaped nose and a raised flange at the base, as shown in Figure 2.7. This type of projectile is usually fired from a powder burning gun. This type of projectile has been used widely by military agencies and personal armor manufactures for ballistic performance studies (Bhatnager et al., 1989; Kang and Lee, 1994; Lin and Bhatnager, 1992; Bless and Hartman, 1989; Cuniff, 1992).

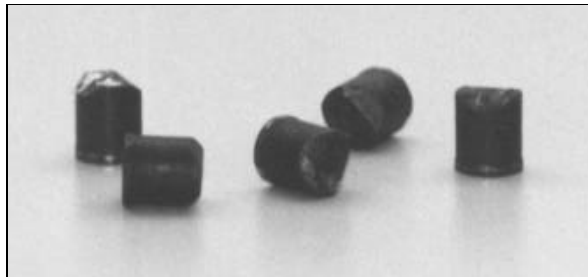


Figure 2.7: Photo of fragment simulated projectiles.

Commercially available ammunition is used for testing at ballistic velocities with a burning powder firing device (Lin et al., 1988). Projectiles of this type are used because they are inexpensive, can be easily obtained (gun and projectiles can be purchased at local sporting goods store), and in some cases may represent the exact type of threat one may be designing for. However, since most commercial ammunition is made of lead, projectile deformation and breakup may be of concern.

2.3.6.3 Method of Analysis

Several different methods of analysis have been used for impact testing at high and ballistic velocities, depending on the type of response desired for the particular threat one is designing for. The large variety of test methods presented in the literature is due to a lack of unified official testing standards which can make the comparison of various results difficult. Test schemes to measure ballistic performance include residual velocity, V_{50} ballistic limit, penetration depth, and instrumented techniques.

For residual velocity testing, the specimen is completely perforated (Lin et al., 1990; Heatherington and Rajagopalan, 1991; Gupta and Madhu, 1992; Jenq et al., 1994). By measuring the velocity of the projectile entering and exiting the specimen, the amount of energy absorbed by the composite E_{absorbed} is calculated as:

$$E_{\text{absorbed}} = \frac{1}{2} m_{\text{projectile}} (V_{\text{in}}^2 - V_{\text{out}}^2) \quad (2.1)$$

where $m_{\text{projectile}}$ is the mass of the projectile and V_{in} and V_{out} are the velocities entering and exiting the specimen, respectively. This type of test method is typically used for residual strength testing where penetration resistance is not required.

V_{50} ballistic limit testing involves determining the velocity at which there is a 50% probability of specimen penetration (Cunniff et al., 1989; Kang and Lee, 1994; Heatherington, 1992; Wright et al., 1993). This can be seen as the velocity at which the projectile just penetrates the composite. According to military specification MIL-STD-662E, testing involves taking a certain number of shots where the projectile penetrates the specimen and that same number of shots where no penetration occurs. If all shots are within a specified velocity range (usually 125 ft/sec) then the V_{50} ballistic limit is calculated from the average of these measurements. This type of testing has been widely used by government agencies and armor manufactures for acceptance testing and material performance rating. Since the extent of damage increases with projectile velocity until the point at which the specimen is penetrated and then decreases as the projectile velocity increases past this point, this test method is good for determining the maximum amount of damage a particular impact threat may incur.

Another method for analyzing resistance to ballistic impact is to measure the depth of projectile penetration (Walters and Scott, 1990; Dikshit et al., 1995; Pageau et al., 1991). When impacting metal armor, characteristics of the penetration cavity is observed to gain insight into the materials impact absorption mechanisms. This method is also useful when comparing several materials to be used in applications where penetration resistance is required.

The amount of information obtained from each of the test methods presented are limited in their ability to explain the dynamics of the impact event. Therefore, novel test methods have been developed to gain more information about the impact event. In order to gain a force vs. time curve, Azzi et al. (1991) created a reverse impact technique where the composite specimen was accelerated to impact a stationary impactor instrumented with a piezoresistive gauge. In another study, Zee et al. (1991) inserted a small magnet on the projectile. The changing magnetic flux in coils placed around the specimen gave a real-time velocity profile during the specimen penetration. These two types of tests are important because they provide more information regarding the energy absorption during the impact process (near the front in shear, in the middle and back through delamination, and near the back through fiber failure).

2.4 Improving High and Ballistic Velocity Impact Damage Resistance

Due to the low strain to failure and low transverse shear strength of the graphite fiber coupled with the brittle nature of the epoxy matrix, graphite epoxy composites have very poor resistance to high energy impact. To date, only limited work has been done in the area of impact resistance improvement of graphite composites subjected to high and ballistic velocity impact.

Some of the methods used to improve low velocity impact resistance are not appropriate in improving the high and ballistic velocity impact resistance. Indeed, the response of composites at low velocities can be very different, as discussed in section 2.2. For the fiber and matrix toughening approach to improved impact resistance, the large amount of material needed for high velocity applications would result in a significant reduction in the structural stiffness of the composite. As for interface toughening and through-the-thickness reinforcements, which are designed to reduce delamination, these methods are effective at higher velocities if penetration resistance is not required and improved structural strength after impact is desired. However, if penetration resistance is required, prohibiting delamination may be counter-effective since delamination plays an important role in energy absorption and stopping the motion of the projectile. Dorey (1974) concluded that the carbon fiber matrix bond strength should be high for good threshold impact performance, but low for projectile containment.

Hybridizing graphite composites with high strain materials is effective for high velocity applications. Through hybridizing, a portion of the energy imparted by the projectile is transferred to the high strain component reducing the amount of energy causing damage to the base composite. Various high strain materials, such as aramid fibers (Kevlar™), S-glass, and high performance polyethylene(Spectra™), have been shown to be effective ballistic resistant materials, which makes them good candidates for hybrid applications (Bless and Hartman, 1989; Lee et al., 1994; Zhu et al., 1991). Dorey (1974) found that hybrid composites faced with Kevlar 49™ performed better than all carbon composites when impacted by a steel ball traveling at ballistic velocities. Another material known for its high strain capabilities is the superelastic shape memory alloy (SMA). As discussed in section 2.1.3, this superelastic SMA has been shown to be effective at low velocities (Kiesling, 1996; Paine and Rogers, 1994), and may be equally effective in high and ballistic velocity applications. The primary goal of this thesis is to

demonstrate the concept of using high strain SMA and ECPE hybrid components to improve the ballistic impact resistance of graphite composites.

Chapter 3

Experimental Procedure

3.1 Objectives and Approach

The objective of this research is to determine the effect of adding shape memory alloy fibers and high performance extended chain polyethylene fiber hybrid components on the ballistic impact (1000+ ft/sec) resistance of graphite epoxy composites. Methods for improving the composite resistance to complete penetration without a significant increase in weight or volume is the primary interest of this study. Of secondary interest is the ability of the hybrid component to improve the composites structural strength after impact. By performing ballistic tests on various configurations of hybrid graphite specimens, increases in energy absorption due to the hybrid components will be determined.

In this thesis, the experiments are designed to have testing conditions similar to actual ballistic applications. This is accomplished by impacting large specimens (12" x 12") instead of the common one dimensional clamped beam configuration. Although one can visually identify damage modes easily along the length of a beam specimen, the results differ from larger two dimensional applications. Also, to create realistic test conditions, the firing device and projectiles are similar to those used by law enforcement officers.

The approach used to determine the energy absorption increase due to the various hybrid components will be to compare the maximum energy absorption capacity of the hybrid graphite composite to that of the plain graphite. Also, inspection and analysis of the impacted specimens will be made to gain an understanding of the characteristics of an effective ballistic impact resistant hybrid component.

3.2 Specimen Fabrication

3.2.1 Control Specimens

A series of tests were performed on plain graphite composite specimens as a baseline against which the hybrid composites will be compared. Square 12" X 12" panels were fabricated using graphite/bismaleimide double ply prepreg (0.01" thick) from BASF Corporation (G40-600/5245c). The panels were cured at a pressure of 85 psi in an MTP-24 Smart Press according to manufacturers recommendations as shown in Figure 3.1. A C-scan of one of the panels showed good lamina consolidation.

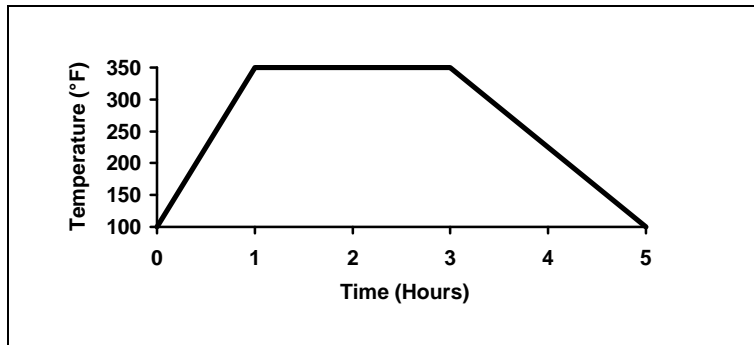


Figure 3.1: Cure cycle used in the fabrication of composite panels.

Preliminary tests were performed on panels of various thickness to determine the number of plies necessary to prevent projectile penetration near the lower end of the velocity range of the firing device (900 ft/sec). Using this approach, graphite composite panels with twenty layers in a $0^{\circ}/90^{\circ}$ cross-ply configuration (.22" thick) were selected for control specimen testing.

3.2.2 SMA Hybrids

The first hybrid composite configuration studied had 0.015" diameter superelastic Shape Memory Alloy fibers embedded at various locations within the composite. The SMA fibers, obtained from Shape Memory Applications Inc., were made of 56% nickel and 44% titanium.

The SMA fibers embedded within the composite were placed between graphite prepreg plies before curing. Since the SMA fibers were parallel to one of the adjacent graphite plies, the SMA fibers were pressed into the thickness of the prepreg upon curing as shown in Figure 3.2.

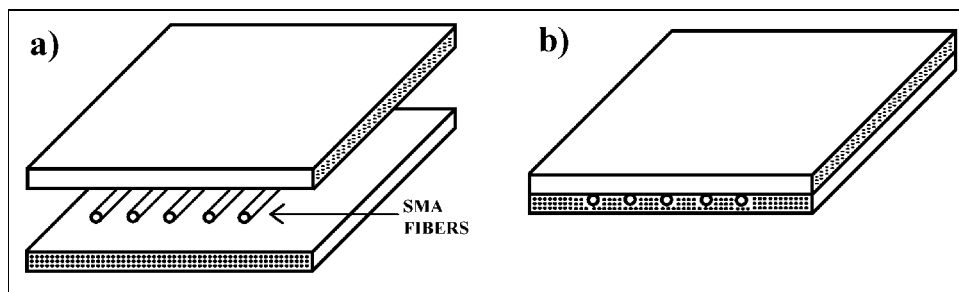


Figure 3.2: Schematic demonstrating how SMA is embedded in graphite composite; a) Layup before consolidation b) Layup after consolidation.

3.2.3 SMA-Kevlar Weave

Based on a low velocity impact study performed on SMA graphite hybrids, it was anticipated that there would be problems with the SMA fibers being pushed aside as the projectile penetrated the composite (Kiesling, 95). If such a situation were to exist at ballistic velocities, it would be difficult to properly determine the full potential of the SMA as an effective ballistic impact resistant material.

In order to prevent SMA fiber separation, bi-directional SMA weave and Kevlar-SMA weave configurations were explored. Weaving was performed on a hand loom using a plain weave pattern. Due to the superelasticity of the SMA and its inability to crimp, it was difficult to fabricate a bi-directional SMA weave with a close mesh. Thus, the bi-directional SMA weave was not used in ballistic testing. However, it was possible to weave the SMA with a more flexible fiber that could crimp fairly easily in the other direction as shown in Figure 3.3. The intent of the flexible fiber was to provide enough axial and shear strength to prohibit the penetrating projectile from pushing the SMA fibers aside. Kevlar™, an aramid from DuPont, was chosen as weaving material for its excellent strain and shear properties. Furthermore, Kevlar™ can be embedded within the graphite composite because of its compatibility with the epoxy resin and the cure cycle. Graphite was not selected as weaving fibers because of its relatively low strain to failure and its extremely low shear strength which would provide little support in the prevention of SMA separation, even though it would have reduced the amount of experimental variables.

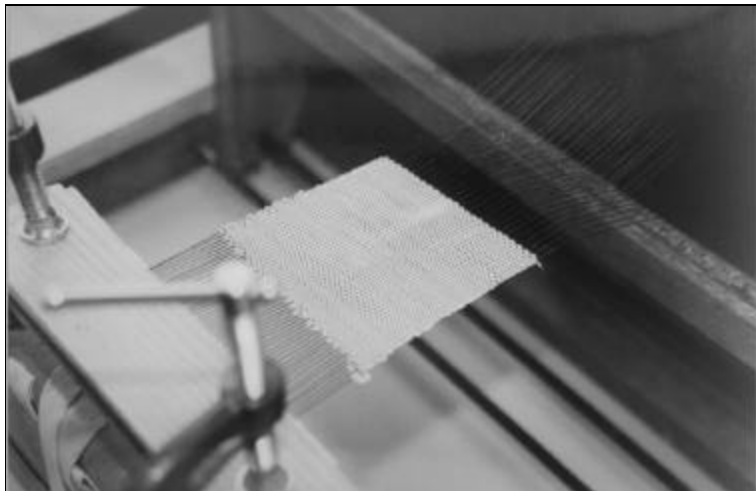


Figure 3.3: Photo of weaving loom with SMA-Kevlar configuration.

3.2.4 Attaching ECPE Components

The third hybrid composite configuration studied had high performance extended chain polyethylene (ECPE) fiber prepreg, known as Spectra Shield™ obtained from Allied Signal, applied to the back face of the graphite panels. The prepreg consists of a thermoplastic rubber resin holding a layer of Spectra 1000™ fibers.

Since the ECPE fiber prepreg's maximum cure temperature is around 270 °F and the graphite epoxy prepreg cures at 350°F, it was necessary to perform specimen fabrication in two steps. The first fabrication step is to prepare a plain graphite composite panel, as discussed in section 3.2.1. The second fabrication step consist of applying the ECPE prepreg to the graphite. In order to obtain a good bond between the graphite and ECPE prepreg, a thermoplastic rubber (Kraton™) diluted with a polymer solvent (cyclohexane) to create a type of “glue” was applied to the surface. Once the applied Kraton™ was dry, several layers of ECPE prepreg were placed on the graphite composite. The entire hybrid panel was then consolidated in a hydraulic press (445 psi) following the manufacturers recommended press cycle, shown in Figure 3.4.

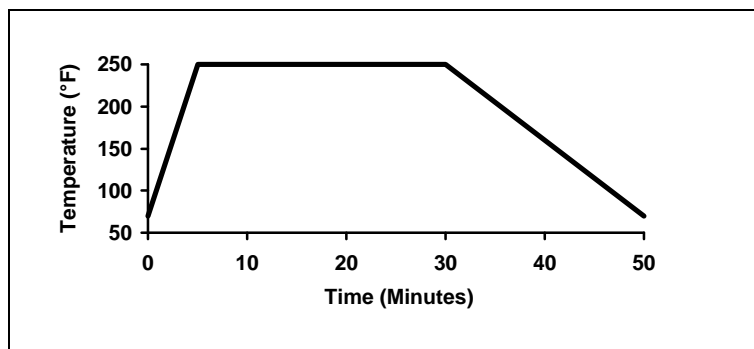


Figure 3.4: Cure cycle for ECPE prepreg.

To validate this two step fabrication process, preliminary tests were performed on a hybrid panel. A very effective bond at the graphite-ECPE interface was observed under ballistic impact. Hybrid delamination only occurred between subsequent ECPE layers.

3.2.5 Embedding SMA in ECPE

The final hybrid configuration studied involved embedding SMA fibers between layers of ECPE prepreg which were then attached to the graphite composite, as discussed in section 3.2.4. However, because of the ECPE prepreg's small thickness (0.007") compared to the SMA fiber diameter (0.015"), the ECPE could not properly consolidate between the SMA fibers; as was the case when embedding the SMA in the graphite prepreg (Figure 3.2). In order to insure proper consolidation, a 1/8" thick sheet of rubber was place on top of the ECPE-SMA layers before being pressed. The aided in pushing the ECPE between SMA fibers in order to create a better bond.

3.3 Test Method

3.3.1 Military and NIJ Standards for Ballistic Impact Testing

The ballistic testing was performed according to the U.S. Military and National Institute of Justice (NIJ) standards (MIL-STD-662E, NIJ Standard 0108.01). These

standards are widely used by government agencies and armor manufacturers for product acceptance testing. The energy absorption values for various hybrid configurations can be obtained using these standards.

Due to the exploratory nature of this research, these test standards were chosen because they enable the user to gain an understanding of the aspects of how to improve the ballistic impact resistance of various systems without requiring a large amount of costly test samples. Also, as mentioned in section 2.2.5, these standards test for the maximum degree of damage a particular projectile can incur.

Testing according to these standards do, however, have their limitations. Because they are based on a limited amount of data points, it is difficult to acquire results with a good statistical significance. Also, the standards lack a method for obtaining dynamic information that may help explain the impact event. Damage characterization is limited to energy absorption values and post impact inspection.

3.3.2 Experimental Setup

The experimental setup was created according to guidelines given in the NIJ standard, as shown in Figure 3.5.

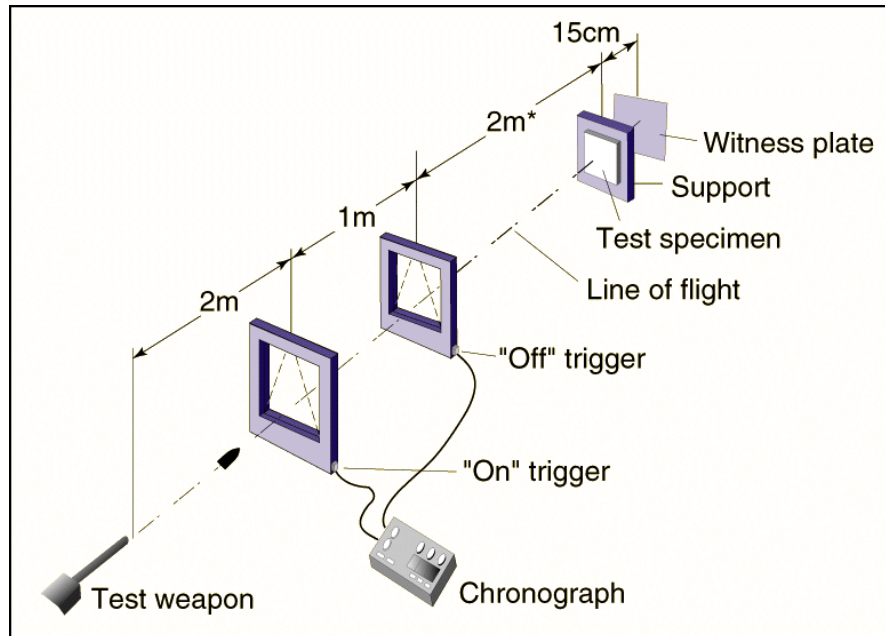


Figure 3.5: Schematic of ballistic test setup following the NIJ standard.

The test weapon was a 9mm Beretta handgun made by Beretta U.S.A. Corp. The gun was mounted in a Ransom Rest™ from Ransom International Corporation with a laser sight attached for accuracy in firing as shown in Figure 3.6.



Figure 3.6: The 9mm handgun was mounted and a laser sight was used to provide maximum accuracy.

The chronograph, which is used to determine the velocity of the projectile, was purchased from Oehler Research (Model 35P).

The test specimens were rigidly clamped between two steel frames. Bolts at the corners and mid-sections of the steel frame were tightened to insure a rigid mount on all four edges of the test specimen. A half of an inch of material was clamped around the perimeter of the test specimens. These two steel frames were attached to a support structure as shown in Figure 3.7. The test specimen was perpendicular to the line of flight of the bullet at the point of impact. Located 6" behind the specimen was a 0.02" thick 2024 T3 aluminum alloy witness plate used to record specimen penetration.

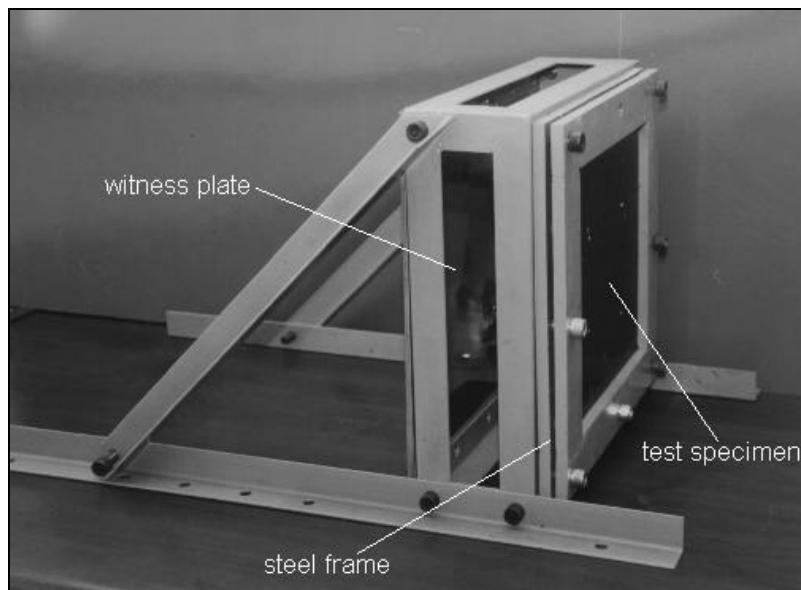


Figure 3.7: Frame mount with test specimen clamped in the front and the witness plate in the rear.

3.3.3 Projectiles

Standard 124 grain (7.45 g) round nose lead projectiles with a copper outer coating (jacket) typically used in a 9mm handguns were used (Figure 3.8). The projectiles, obtained from Hornady Manufacturing Co., had a weight variance less than 1% ($\pm .01$ g).

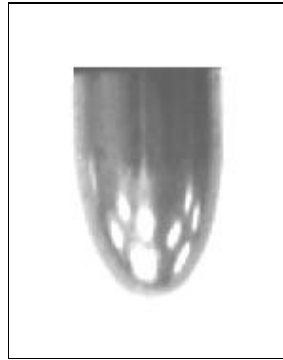


Figure 3.8: Lead projectiles with a copper jacket were used for testing.

3.3.4 Projectile Deployment

The projectile velocity was controlled by altering the weight of propellant (burning powder). Bullseye® smokeless pistol powder from Hercules Inc. was used as the propellant. A series of ammunition tests were initially performed to develop a charge weight vs. velocity curve to be used in subsequent firings.

3.3.5 Test Procedure

The test procedure used to determine the energy absorbed by the hybrid composite panels is now presented. Three panels were constructed for each hybrid configuration and each panel was impacted with four projectiles, as shown in Figure 3.9. The locations for projectile impact was chosen to minimize the effects of previous impact damage and of boundary conditions.

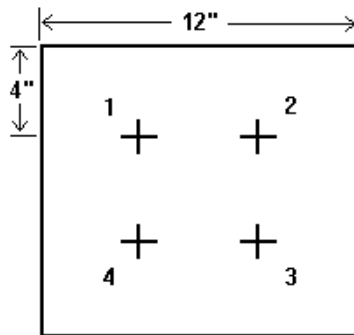


Figure 3.9: Sketch of impact locations and firing order for specimen testing.

The value of four impacts per specimen was chosen as a balance between the fabrication time and cost, and the ability to get results unaffected by previous impacts. Although there might have been some overlapping of impact damage, no correlation between the penetration velocities and the impact order was observed. Data was rejected for cases where significant overlapping of impact damage occurred.

Testing for each hybrid configuration begins with firing a projectile at an estimated velocity that would barely penetrate the specimen. If any fragment of the projectile or specimen creates a hole in the aluminum witness plate allowing light to shine through, then it constitutes a complete penetration (NIJ Standard 0108.01). If no hole exists, it is considered a partial penetration. The next projectile is fired with a higher velocity if the previous projectile resulted in a partial penetration and with a lower velocity if the previous projectile resulted in a complete penetration. This procedure is repeated to obtain progressively smaller differences between partial and complete penetrations until all twelve shots have been fired. An equal number of complete and partial penetrations within a velocity span of 125 ft/sec must be obtained.

3.3.6 Determination of the V_{50} Ballistic Limit

The V_{50} ballistic limit is defined as the velocity at which there is a 50% probability of specimen penetration. This represents the velocity at which the projectile barely penetrates the specimen. Two methods were used to determine the V_{50} ballistic limit from the test data: Military standard and logistic regression analysis. In order to differentiate between the two types, they will be referred to as the military V_{50} ballistic limit and the logistic regression V_{50} ballistic limit in this thesis.

3.3.6.1 Determination of the Military V_{50} Ballistic Limit

The military standard MIL-STD-662E was created by the army to provide a simple cost effective method for determining the V_{50} ballistic limit. It is determined by taking the average of an equal number of highest partial penetration velocities and lowest complete penetration velocities which occur within a specific velocity range for a particular specimen configuration. The velocity range requirement is necessary since an unusually high or low data point could offset the average, causing a misrepresentation of the V_{50} ballistic limit. According to standard recommendations, five partial and five complete penetrations within a 125 ft/sec range was set as the criteria for testing.

This method has the advantage of being simple and cost effective since it does not require sophisticated statistical analysis and only 10 shots are needed. However, results may be effected by the users choices of velocities. Also, when testing, some data points may have to be rejected if they fall outside the velocity range requirement.

3.3.6.2 Determination of the Logistic Regression V_{50} Ballistic Limit

Logistic regression is a method of statistical analysis used in engineering, biological, and health science applications where there are only two possible outcomes for a given test. For this study, a 0 or 1 value was assigned to a data point depending on if it was a partial or complete penetration. Data is then fit to a logistic regression model given by:

$$P = \frac{1}{1 + e^{-(a + b*v)}} \quad (3.1)$$

where P is the probability of an event happening at a certain velocity v . The variables a and b are determined by logistic regression fitting which involves an iterative matrix solution of which the details are presented by Myers (1990). With $P=0.5$ and solving for v in Equation 3.1., the V_{50} becomes;

$$V_{50} = \frac{-a}{b} \quad (3.2)$$

For this study, a statistical software package called SPSS from SPSS Inc. was used to determine the values of the variables a and b . The general shape of a probability curve generated from logistic regression analysis of a data set is shown in Figure 3.10.

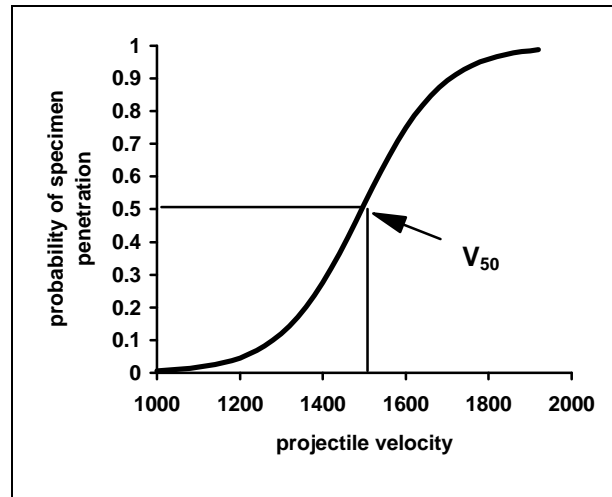


Figure 3.10: Example demonstrating the general shape of a probability curve generated from logistic regression analysis of a data set.

The advantage of using logistic regression analysis is that V_{50} ballistic limit results are not as sensitive to the users choice of velocities. As shown in Figure 3.10, the slope of the curve near the 0% and 100% probability approach zero. Thus, an extremely high or low velocity measurement will not offset the V_{50} calculation as is the case with the military standard method.

The disadvantage of logistic regression analysis is that a large number of data points is required for a proper curve fit. Since only 12 data points are obtained from each hybrid configuration, confidence intervals are unobtainable, providing no guarantee that results are accurately represented.

3.3.7 Calculation of Energy Absorption Values

For each of the hybrid configurations, the energy absorbed by the composite was taken as the metric for impact penetration resistance. From the V_{50} ballistic limit, the amount of energy E absorbed was calculated as:

$$E = \frac{1}{2} * m_p * V_{50}^2 \quad (3.3)$$

where m_p is the mass of the projectile. To determine the effectiveness of the hybrid component in improving the impact penetration resistance, the variations in energy absorbed with respect to the plain graphite composite specimen will be used. Percent changes in energy absorption $\% \Delta E$ was then calculated as:

$$\% \Delta E = \frac{E - E_c}{E_c} * 100 \quad (3.4)$$

where E_c is the energy absorbed by the control specimen.

Chapter 4

Experimental Results

Plain graphite specimens were first tested in order to set the basis for comparison when testing subsequent hybrid configurations. Next, in order to determine the most appropriate location for a hybrid component, specimens containing a small amount of uni-directional SMA fibers embedded in the front, middle, and backface locations were tested. Upon concluding that the backface was the most appropriate location, bi-directional SMA, aramid SMA weave, and increased volume fraction uni-directional SMA layer specimens were tested. Various amounts of ECPE were also tested on the backface. Finally, combinations of SMA and ECPE components were placed on the backface of the graphite composite and tested in order to observe if the SMA fibers performed better in a more strain compatible system. From the results of all of the hybrid configurations, energy absorption comparisons were made.

4.1 Plain Graphite Specimens

The objective of the plain graphite specimens was to observe ballistic impact damage mechanisms and to determine the maximum amount of energy that can be absorbed by the projectile (V_{50} ballistic limit) in the absence of hybrid components. Other important observations made while testing the plain graphite specimens included the projectile deformation and the effect of using four shots per panel.

4.1.1 Impact Damage Mechanisms

The observed mechanisms for absorbing ballistic impact included shear plug, matrix cracking, delamination, and fiber failure. A diamond saw was used to cut specimens across the impact point in order to observe damage modes (Figure 4.1) which were consistent with observations made in existing literature, as discussed in section 2.1.1 and 2.3.2.

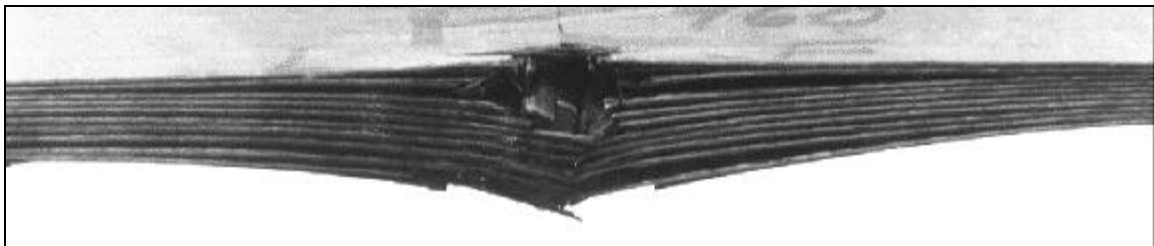


Figure 4.1: Graphite specimen impacted near its V_{50} ballistic limit shows a combination of shear plug, matrix cracking, delamination, and fiber failure.

Unlike low velocity impact, the energy of the projectiles traveling at ballistic velocities were sufficient to create a shear plug near the front face of the composite. It was observed that the diameter of the shear plug was close to the diameter of the projectile on the first ply and then increased slightly with depth (see Figure 4.2). The depth of the shear plug appeared to be dependent on the velocity of the projectile. For panels impacted near the V_{50} ballistic limit, such as the one in Figure 4.2, the shear plug depth tended to be about half of the specimen thickness (10 out of 20 plies).

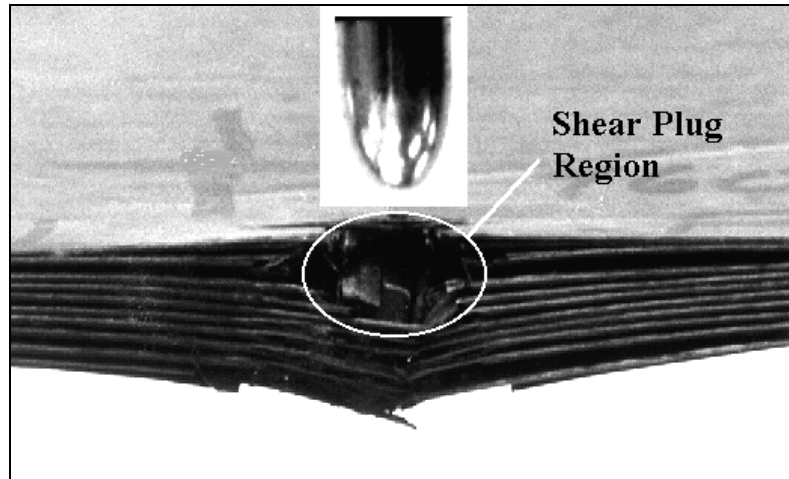


Figure 4.2: Photo of projectile and photo of specimen impacted near its V_{50} ballistic limit pointing out shear plug region. Note: Photos are at same scale.

Delamination between plies was observed through the thickness of the composite. The delaminations were large near the front face, reduced in the mid region, and then gradually increased towards the back face where damage was most severe. This is pointed out in the photo shown in Figure 4.3. It is believed that the delamination near the front face of the composite was due to the initial shock wave created upon impact. Shortly after this initial region, the extent of delamination was reduced to its minimum since the primary damage mode was through the creation of the shear plug. As shown in Figure 4.3, the extent of delamination past the shear plug region increased with depth, being most severe at the backface. It is the opinion of the author that this occurred since, as the velocity of the projectile decreases as it penetrates the composite, the graphite fibers have increasingly more time to fail. Therefore, the time for delaminations to propagate outwards increases with depth in the composite. These results are consistent with observations made by Cantwell and Morton (1990a).

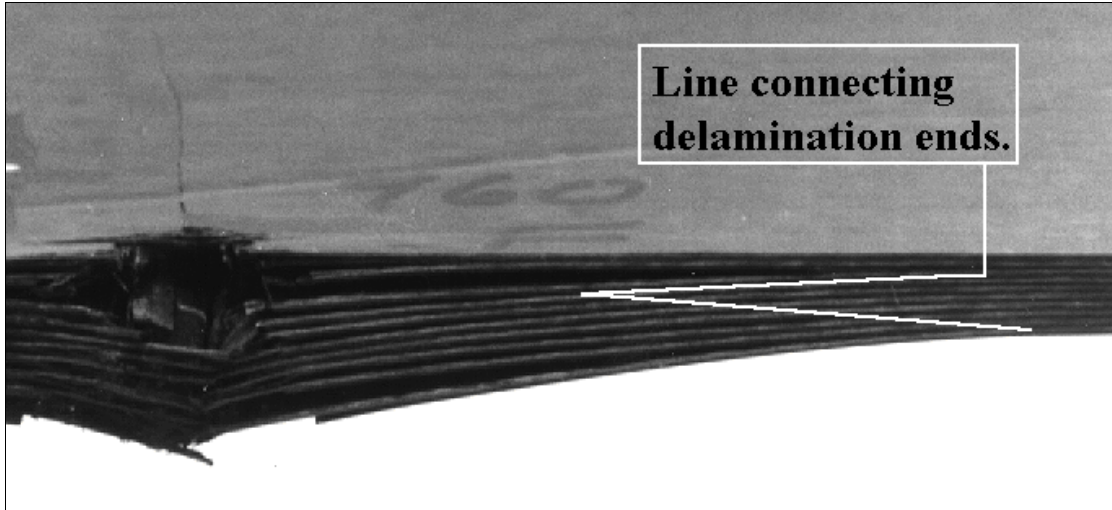


Figure 4.3: Photo of a graphite specimen impacted near its V_{50} ballistic limit pointing out delaminations ends.

4.1.2 Determination of the V_{50} Ballistic Limit for Plain Graphite Specimens

The V_{50} ballistic limit for plain graphite specimens was determined for subsequent comparisons with the hybrid configurations. Four panels were used to obtain data points making a total of sixteen shots. The highest five partial penetrations and lowest five complete penetrations were used to determine the military V_{50} ballistic limit of 959 ft/sec. The difference between the highest complete penetration and the lowest partial penetration was 113 ft/sec, which is within the 125 ft/sec requirement. Data points are shown in Figure 4.4. A logistic regression V_{50} ballistic limit of 965 ft/sec was calculated.

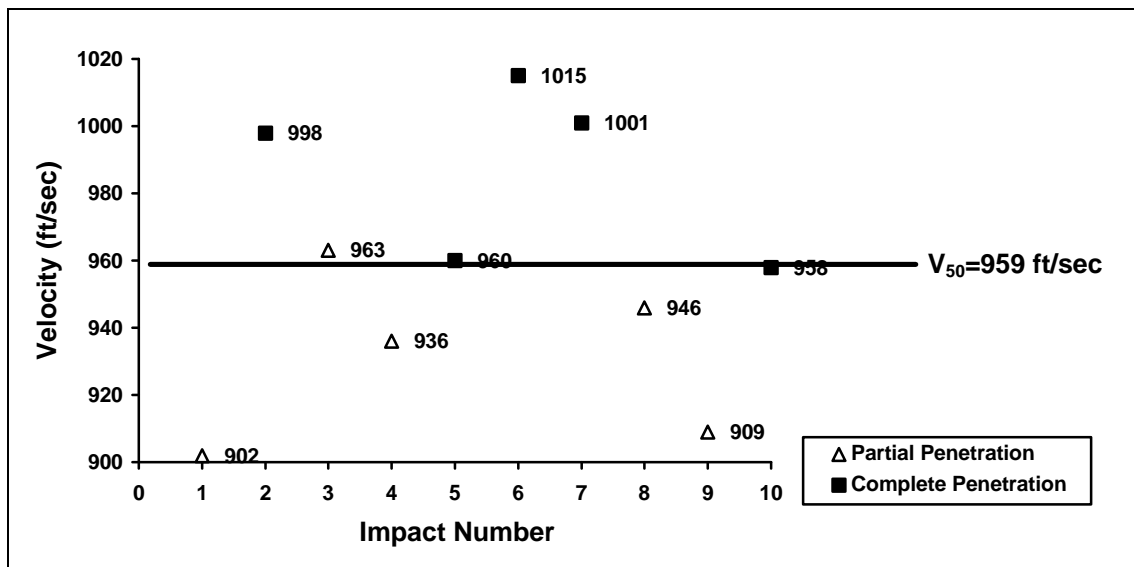


Figure 4.4: Graphical representation of data points used to determine the military V_{50} ballistic limit for plain graphite composites.

In three of the plain graphite specimens tested, an additional projectile was fired in the center of the four previous shots to observe the effect of overlapping damage on penetration. From the results, the overlapping damage does not appear to have a significant effect on penetration velocity (Table 4.1).

Table 4.1: Results of a fifth shot in three of the plain graphite specimens.

Panel	Velocity	Result
1	956 ft/sec	Partial Penetration
2	1011 ft/sec	Complete Penetration
3	954 ft/sec	Complete Penetration

4.1.3 Projectile Effects

Significant projectile deformation was observed when testing plain graphite specimens. Projectiles would rebound backwards with deformed shapes, as shown in Figure 4.5, at impact velocities below the energy level required to penetrate the front face.

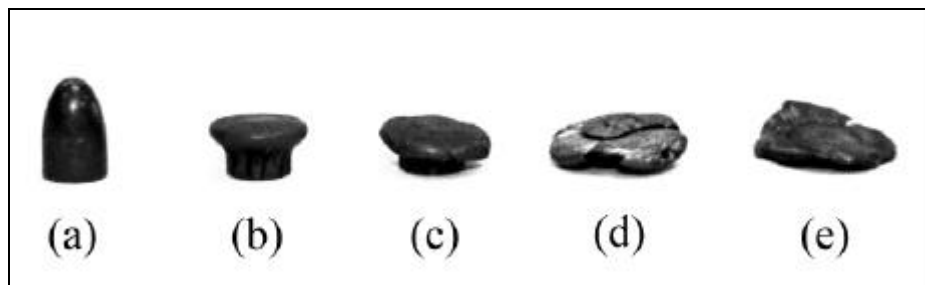


Figure 4.5: Projectile deformations below first ply penetration level; (a) 0 ft/sec (b) 605 ft/sec (c) 665 ft/sec (d) 781 ft/sec (e) 833 ft/sec.

For projectiles traveling at a velocity sufficient to perforate the first ply, the deformation was very different. The copper jacket was typically peeled off near the front of the specimen while the remaining randomly deformed lead portion made its way through the rest of the composite. The shape and remaining mass of recovered projectiles were found to be random in nature and often contained sharp edges, as shown in Figure 4.6.



Figure 4.6: Various deformed projectiles after specimen penetration.

4.1.4 Effect of Four Shots Per Panel

The C-scan of an impacted panel, shown in Figure 4.7, reveal the diamond shaped delamination pattern commonly observed in cross-ply laminates impacted at ballistic velocities (Cristescu et al, 1975). As discussed in section 3.3.5, the choice of four shots per panel was chosen as a balance between the fabrication time and cost, and the ability to get results unaffected by previous impacts. From visual and C-scan observations, it is the opinion of the author that the choice of four shots per panel was suitable.

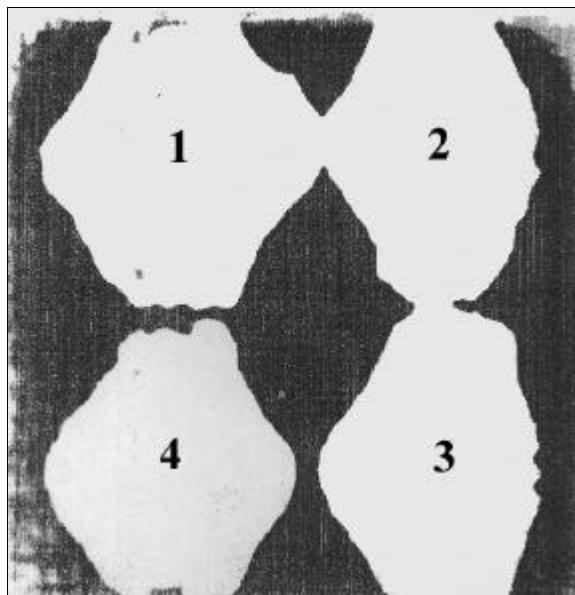


Figure 4.7: C-scan of a graphite panel impacted in numbered order showing extent of delamination (white region represents areas of delamination).

Some overlapping damage between successive impacts and edge effects did exist, as can be seen in Figure 4.7, but their effect on the energy absorption values appeared to be minimal.

4.2 SMA Location Tests

Tests were performed in order to gain an idea of the most suitable SMA fiber location within the composite. For this purpose, three hybrid configurations were tested where one uni-directional layer with a 1/16" spacing, corresponding to a 1.2 % SMA volume fraction, was embedded on the front face, in the middle, and on the backface of the graphite composite.

4.2.1 SMA Front Face Tests

The results for specimens containing one layer of unidirectional SMA fibers on the front face are presented in Figure 4.8.

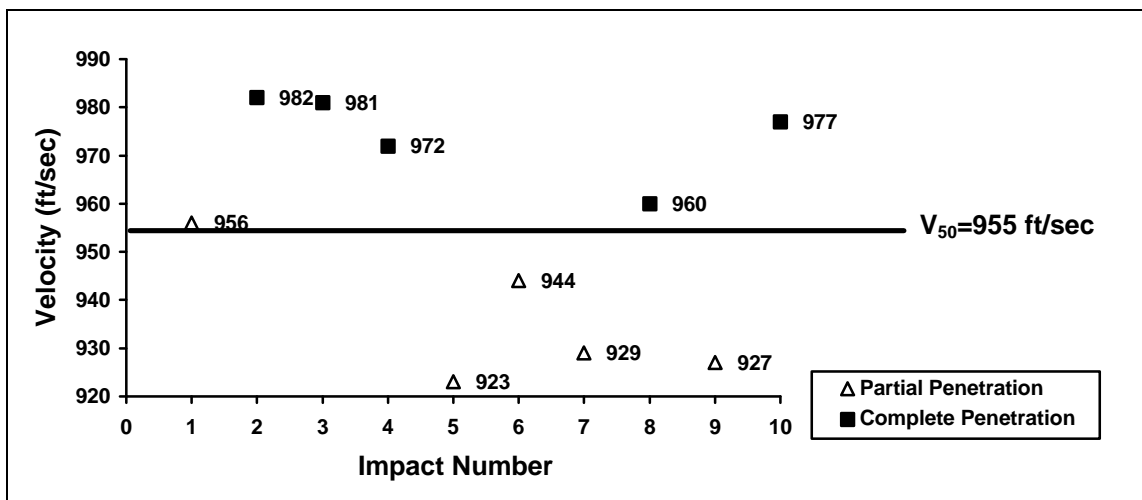


Figure 4.8: Graphical representation of data points used to determine the military V_{50} ballistic limit for specimens with a 1.2 % volume fraction of uni-directional SMA fibers embedded on the front face of the composite.

A military V_{50} ballistic limit of 955 ft/sec was calculated, with a range of 59 ft/sec between all data points. The logistic regression V_{50} ballistic limit was 958 ft/sec. When compared the V_{50} ballistic limit of the plain composites (959 ft/sec), the addition of SMA fibers on the front face appear to have no effect on the energy absorption capacity of the composite. The author has no clear explanation why the V_{50} ballistic limit was not increased, despite the addition of the tough material. This reduction might have occurred since the SMA fibers could have aided in cutting through the rest of the composite while being pushed through by the projectile. Perhaps no increase in energy absorption was found since the SMA was sheared before being allowed to go through its stress induced martensitic phase transformation. The post inspection of the composite shows that the SMA fibers which

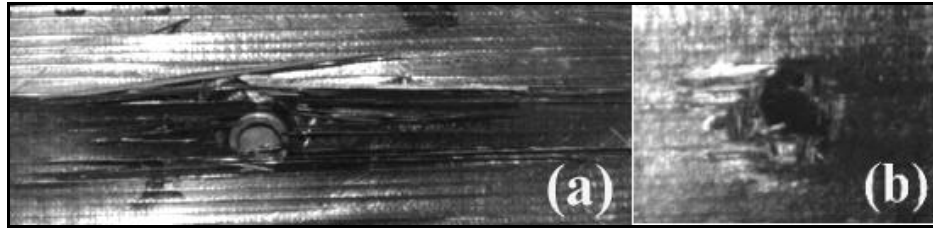


Figure 4.9: Additional damage in the composite is observed with SMA fibers embedded on front face (a) when compared to plain graphite (b).

failed in shear caused additional damage extending outward along the SMA graphite interface (see Figure 4.9).

The increased damage on the front face of the composite should be an indication of increased impact energy dissipation. Since this was not the case, the effect of this additional damage is unclear.

4.2.2 SMA Middle Tests

Results similar to the front face were found with SMA fibers embedded in the middle of the composite. The military V_{50} ballistic limit was decreased to 940 ft/sec when compared to the plain graphite composite (959 ft/sec). Data points are shown in Figure 4.10. The logistic regression V_{50} ballistic limit was 937 ft/sec.

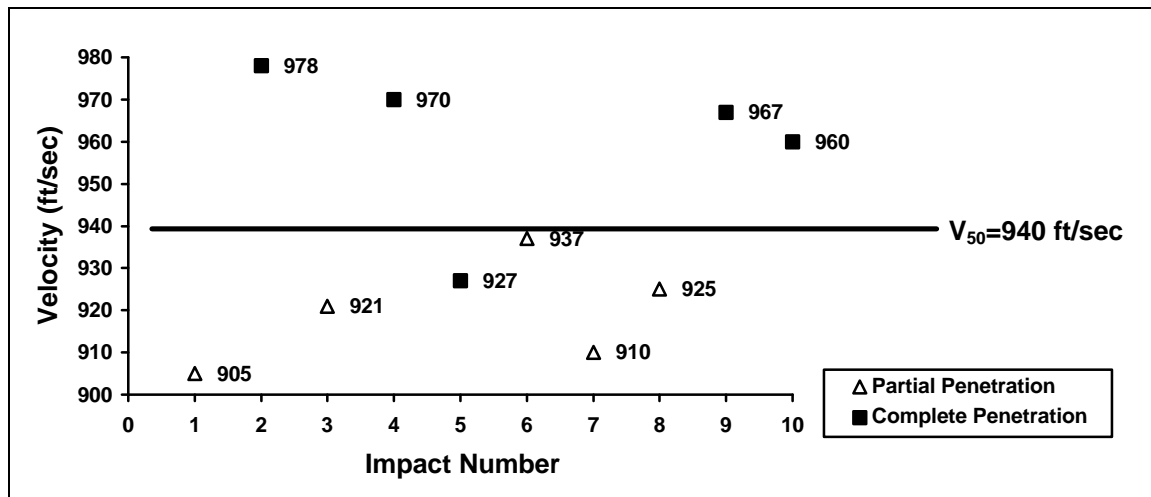


Figure 4.10: Graphical representation of data points used to determine the military V_{50} ballistic limit for specimens with a 1.2 % volume fraction of uni-directional SMA fibers embedded in the middle of the composite.

By cutting the composite across the impact zone with a diamond saw, it was observed that SMA fibers were also broken primarily in shear when impacted at velocities near the V_{50} ballistic limit. Once again, it is unclear why a reduction in the V_{50} ballistic limit was observed. It may be due to reasons similar to those given for the SMA front face tests.

4.2.3 SMA Back Face Tests

A slight improvement in the energy absorbing capacity of the hybrid composite was found from specimens containing a 1.2 % volume fraction of uni-directional SMA fibers embedded on the back face. A military V_{50} ballistic limit of 976 ft/sec was calculated with a velocity range of 83 ft/sec as shown in Figure 4.11. The logistic regression V_{50} ballistic limit was 973 ft/sec. It is believed that this improvement in the ballistic limit was due to the fact that, unlike the front and middle tests, the SMA fibers could be pulled away from the composite and were free to strain in their axial direction. This provided a greater energy absorption capability due to the stressed induced martensitic phase transformation.

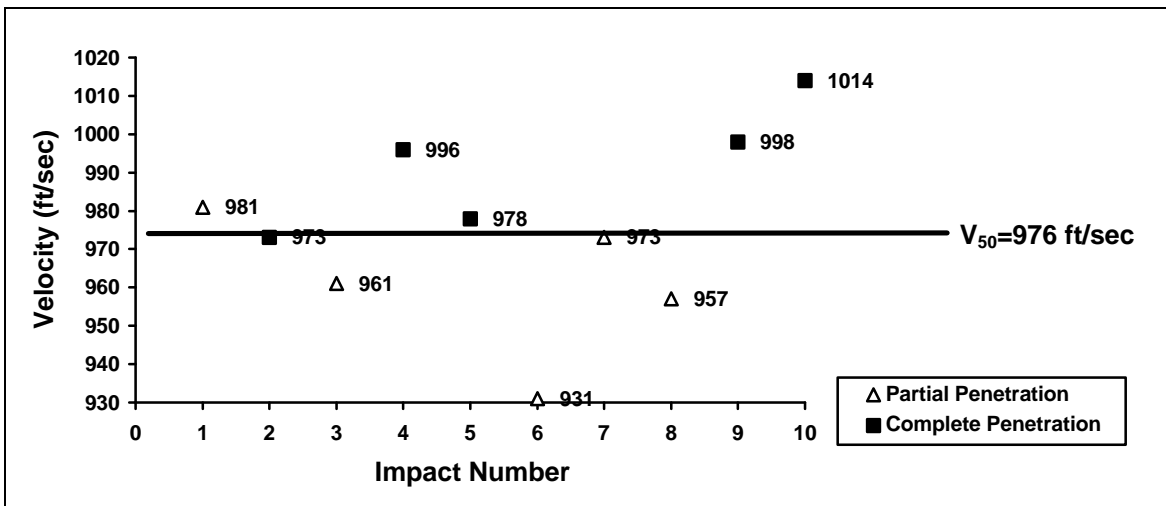


Figure 4.11: Graphical representation of data points used to determine the military V_{50} ballistic limit for specimens with a 1.2 % volume fraction of uni-directional SMA fibers embedded on the backface of the composite.

Although a slight improvement was found, the SMA fibers high strain capabilities were not effectively utilized since none of the SMA fibers were strained to failure. This was due to the existence of severe pullout of the SMA fibers extending to the edges of the specimen. This fiber pullout also aided in degrading the graphite portion of the outermost ply. Furthermore, the SMA fibers located in the path of the projectile were sometimes pushed aside as the projectile penetrated the composite.

It is believed that the severe SMA fiber pullout was due to a strain mismatch between the tough SMA and the brittle epoxy coupled with the extremely short reaction time of the impact event. Furthermore, it is the author's opinion that the principal energy

absorption mechanism responsible for the small increase in the V_{50} ballistic limit can possibly be attributed to the breaking of the SMA-epoxy interface and not to the strain energy mechanisms of the SMA.

4.3 SMA-Aramid Weave Tests

In order to prevent the SMA fiber separation by the projectile, as discussed in section 3.2.3, SMA-aramid weave hybrid components were placed on the backface of the graphite composite. The experimental results indicates that this type of reinforcement was ineffective: The military V_{50} ballistic limit of 944 ft/sec, within a velocity range of 84 ft/sec, is significantly lower than the plain graphite composite value. The logistic regression V_{50} ballistic limit was 945 ft/sec.

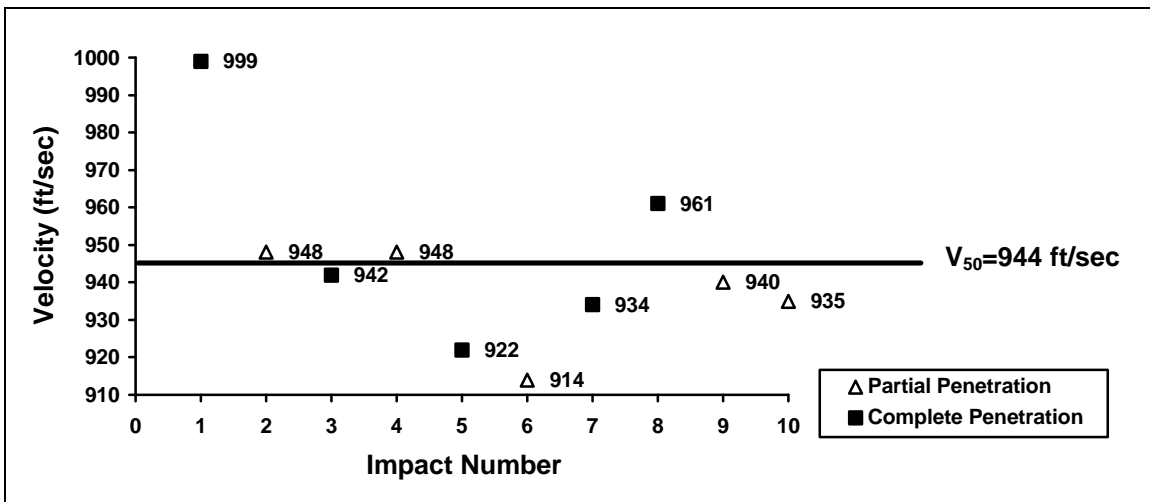


Figure 4.12: Graphical representation of data points used to determine the military V_{50} ballistic limit for specimens with a 1.2 % volume fraction of uni-directional SMA fibers with aramid weave embedded on the backface of the composite.

Various inefficiencies observed with the SMA-aramid weave were responsible for their reduced performance. In most of the penetrated specimens, the deformed projectile would catch and pull out one or two SMA fibers as shown in Figure 4.13. As the SMA fiber was pulled out, it sheared the aramid due to the high stress concentrations created by the SMA fibers. The aramid's resistance to the shearing action of the SMA was affected by the presence of the epoxy. In a study by Hsieh et al. (1990), it was concluded that Kevlar™ (aramid) fibers cannot be fully utilized due to the restrictions imposed by the presence of the epoxy matrix. Also responsible for the SMA-aramid hybrid poor performance was the low interfacial bond strength at the SMA/aramid-graphite interface. For impacts near the V_{50} ballistic limit, gross delamination existed at this interface extending to the edges of the specimen (see Figure 4.13).

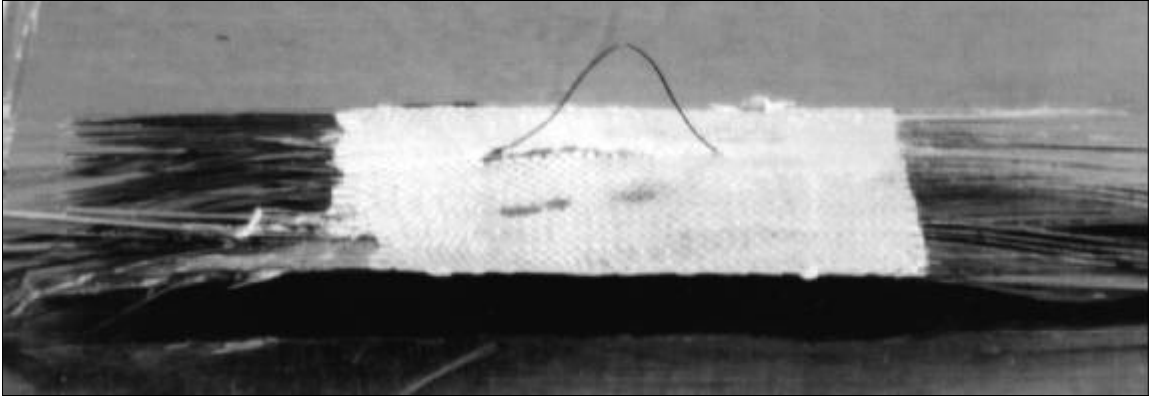


Figure 4.13: Photo of the backface of an impacted specimen containing a SMA-aramid weave hybrid component demonstrating single fiber shear pullout and poor interfacial bond.

4.4 SMA Bi-directional Tests

The effect of adding two perpendicular layers of SMA fibers on the backface of the composite was determined. It was anticipated that there would be an improvement in the energy absorption since twice the amount of SMA fiber (2.4% SMA volume fraction) with reinforcement in both directions was added to the composite. Contrary to this expectation, no increase in energy absorption when compared to the uni-directional case was observed. A military V_{50} ballistic limit of 957 ft/sec was calculated within a velocity range of 73 ft/sec as shown in Figure 4.14. The logistic regression V_{50} ballistic limit was 959 ft/sec.

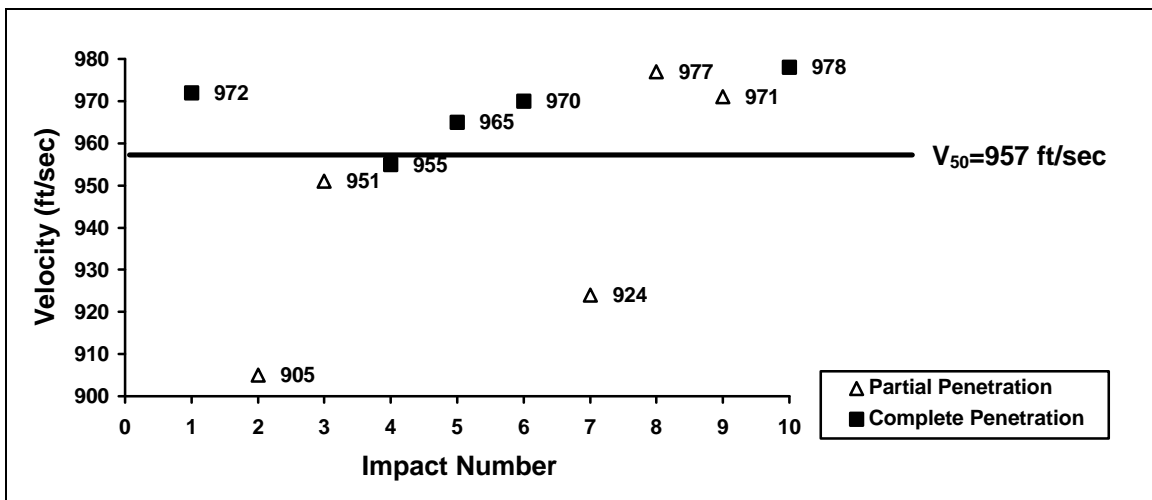


Figure 4.14: Graphical representation of data points used to determine the military V_{50} ballistic limit for specimens with 2.4% volume fraction bi-directional SMA fibers embedded on the backface of the composite.

Unlike the uni-directional case where the SMA was pulled away from the composite along its entire length, the first layer of SMA fibers encountered by the projectile were prohibited from pulling away by the second SMA layer. Therefore the fibers were pulled through a much smaller region (about one inch) causing the “loops” as shown in Figure 4.15. It was also observed that the amount of gross damage incurred to the back plies was greater for the bi-directional SMA case when compared to uni-directional tests.



Figure 4.15: Photo of "loops" created by an SMA layer when impacted by a projectile.

4.5 Increased Volume Fractional Tests

Since the previous tests indicated that uni-directional SMA fibers located on the backface appeared to perform better than the bi-directional fibers, an increased volume percent uni-directional configuration was tested. Due to cost constraints only one panel containing a 4.8% SMA volume fraction (no space between SMA fibers) was fabricated and tested. The experimental results, as shown in Table 4.2, indicate no significant increase in performance. The fact that the energy absorbing capacity of the composite did not improve with a significant increase in SMA fibers supports the notion that the SMA was not being fully utilized due to the strain mismatch between the epoxy and the SMA coupled with the extremely short reaction time.

Table 4.2: Data from specimen containing 4.8% SMA volume fraction embedded on backface.

IMPACT NUMBER	VELOCITY	RESULT
1	987 ft/sec	complete penetration
2	956 ft/sec	complete penetration
3	991 ft/sec	complete penetration

4.6 ECPE Backface Tests

Three, six, and nine layers of ECPE fiber prepreg were tested on the backface of graphite composite specimens. The experimental results are presented in Figures 4.16-18 for the three, six, and nine ECPE layer cases respectively.

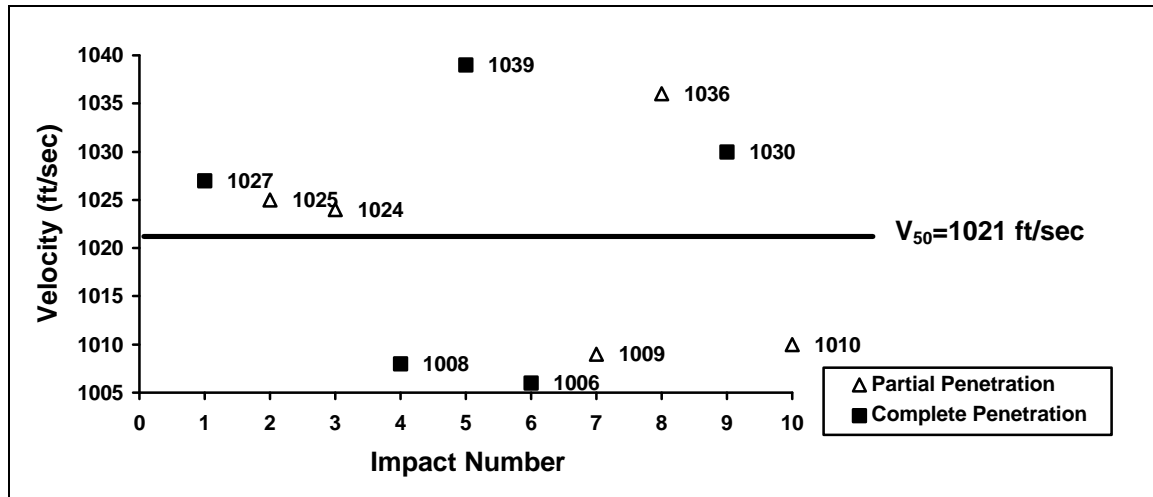


Figure 4.16: Graphical representation of data points used to determine the military V_{50} ballistic limit for specimens with three ECPE prepreg layers bonded to the backface of the composite.

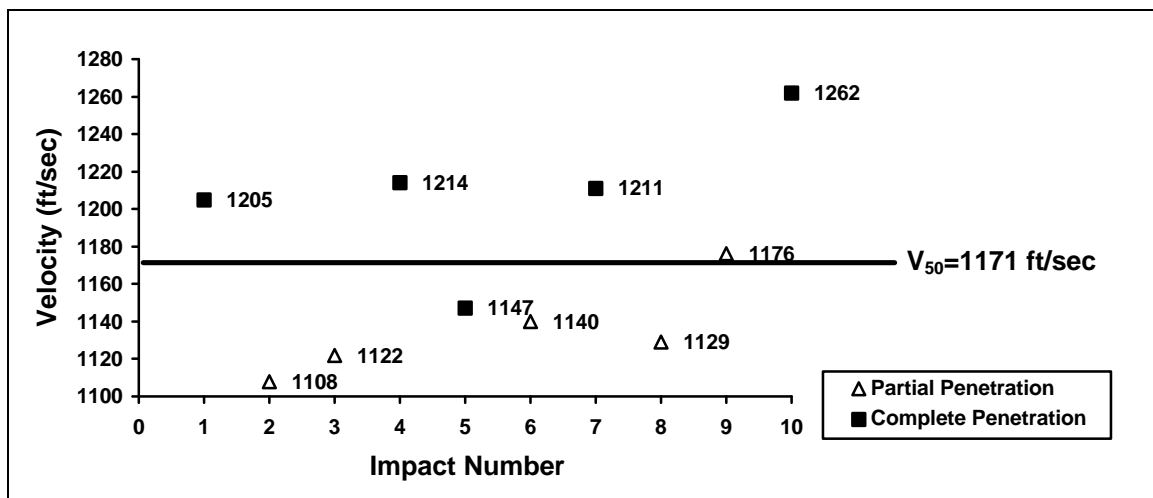


Figure 4.17: Graphical representation of data points used to determine the military V_{50} ballistic limit for specimens with six ECPE prepreg layers bonded to the backface of the composite.

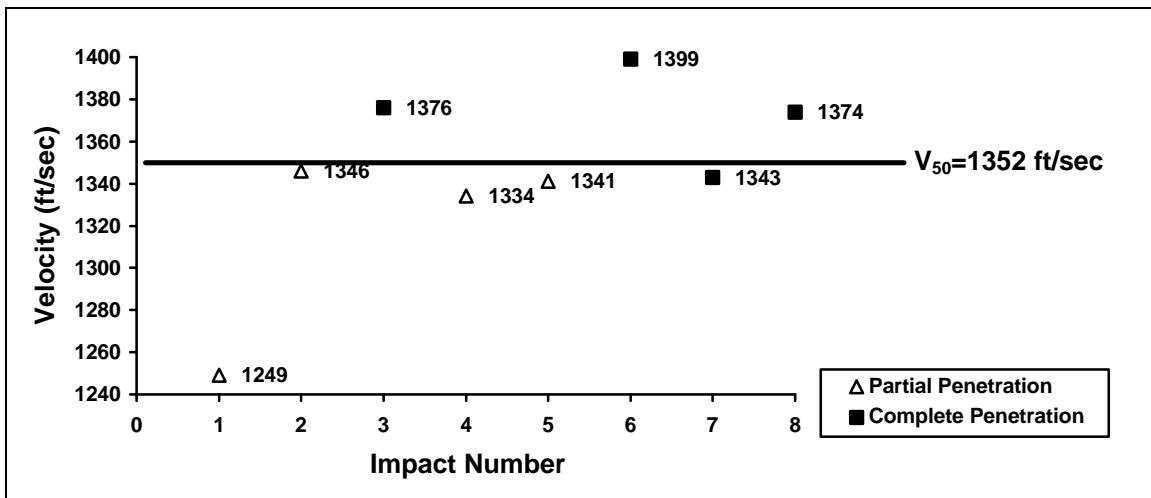


Figure 4.18: Graphical representation of data points used to determine the military V_{50} ballistic limit for specimens with nine ECPE prepreg layers bonded to the backface of the composite.

It should be noted that for the three ECPE layer case, there are three partial penetrations above the calculated V_{50} and two complete penetrations below. However, since the velocity range is low (33 ft/sec), this type of mixture of results can be expected. Also, due to the difficulty of testing at higher velocities, the range of data collected for the six and nine ECPE cases (154 and 150 ft/sec) were above the 125 ft/sec requirement and only eight data points were collected for the nine layer case.

Significant improvements in energy absorption was observed. The military V_{50} ballistic limit values for three, six, and nine ECPE layers were 1021, 1171, and 1352 ft/sec, respectively. The logistic regression V_{50} ballistic limit values for three, six, and nine layers were 1025, 1167, and 1347 ft/sec, respectively.

As shown in the photo of an impacted specimen containing nine ECPE layers (Figure 4.19), the hybrid component was free to strain with greater deformation before failure, thus, effectively absorbing the impact energy. Unlike the previous SMA and Kevlar™ weave cases, the ballistic resistant ECPE material was used to its full potential as evidenced by the existence of fiber strain to failure.



Figure 4.19: The post impact inspection of a specimen containing nine ECPE layers showed large deformation in the ECPE, which contributed to the significant improvement in energy absorption capabilities.

4.7 ECPE-SMA Backface Tests

In order to avoid the strain mismatch problems encountered in previous embedded SMA tests, testing was performed to observe the effect of placing the SMA fibers within the more strain compatible thermoplastic rubber resin of the ECPE prepreg. Two different ECPE-SMA backface configurations were tested. The first configuration included a 1.2% volume fraction layer of SMA fibers (1/16" apart) between the first and second layers of three layers total of ECPE prepreg. The first ECPE layer is bonded to the composite while the third layer is the outer layer. The second configuration has an additional perpendicular layer of SMA fibers between the second and third ECPE layers for a total SMA volume fraction of 2.4%. The ECPE/SMA components were then placed on the backface of the graphite panels.

The calculated military V_{50} ballistic limits for the uni-directional and bi-directional cases (1064 and 1067 ft/sec respectively) were significantly increased when compared to the 3-layer ECPE hybrid case (1021 ft/sec). Data plots are shown in Figures 4.20-21. The logistic regression V_{50} ballistic limit values were 1056 and 1066 ft/sec for the uni and bi-directional cases, respectively. These results suggests that the SMA fibers energy absorbing capabilities are better used when embedded in a strain compliant medium. When compared to the previous SMA hybrids, the amount of gross delamination and fiber pullout was significantly decreased in the ECPE-SMA hybrid specimens. Also, it appears that the ability of the projectile to push the SMA fibers aside was decreased.

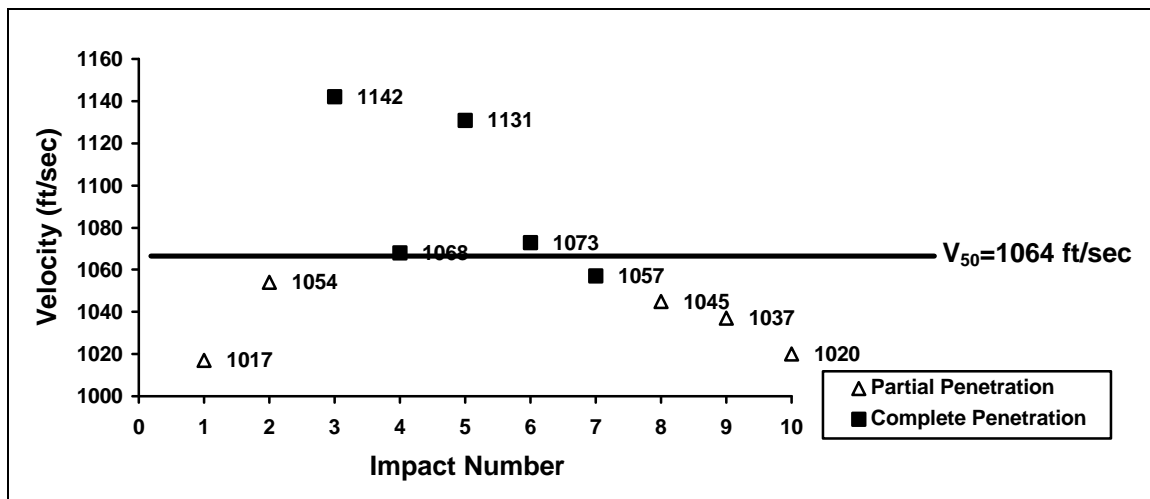


Figure 4.20: Graphical representation of data points used to determine the military V_{50} ballistic limit for specimens with uni-directional SMA and three ECPE prepreg layers on the backface of the composite.

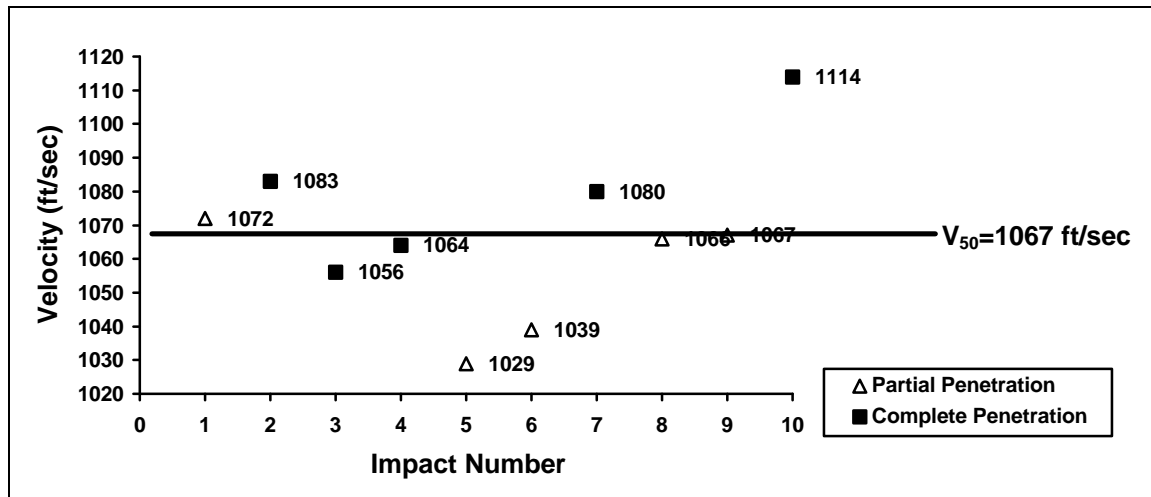


Figure 4.21: Graphical representation of data points used to determine the military V_{50} ballistic limit for specimens with bi-directional SMA and three ECPE prepreg layers on the backface of the composite.

Although improvements in energy absorption were observed in the ECPE-SMA hybrid specimens, the failure mechanisms were similar to the previous SMA hybrid tests. Indeed, failure due to single fiber shear pullout similar to the SMA-aramid weave specimens was observed in the ECPE-SMA uni-directional case as shown in Figure 4.22. Furthermore, the characteristic “loops” observed in the bi-directional SMA specimens were also observed in the ECPE-SMA bi-directional composites as shown in Figure 4.23. Also, the additional perpendicular layer in the bi-directional ECPE-SMA hybrid component did not demonstrate a significant improvement when compared to the uni-directional ECPE-SMA hybrids. Finally, even though the SMA fibers were better used, they were still not fully utilized as evidenced by the non-existence of SMA fibers strained to failure.

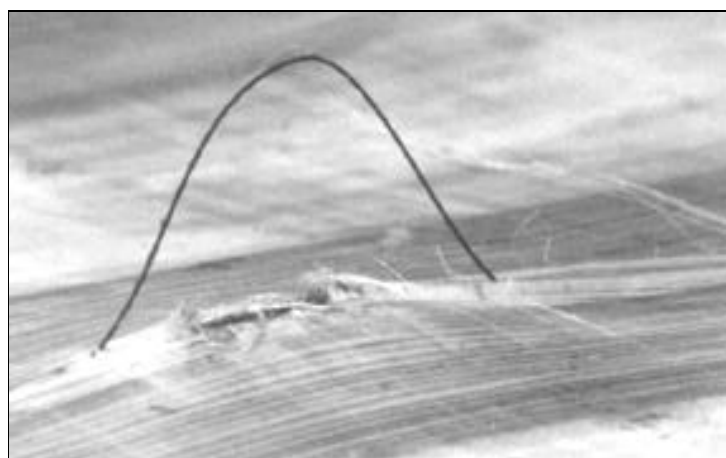


Figure 4.22: Photo of the backface of an impacted ECPE-SMA uni-directional composite specimen demonstrating single fiber shear pullout.

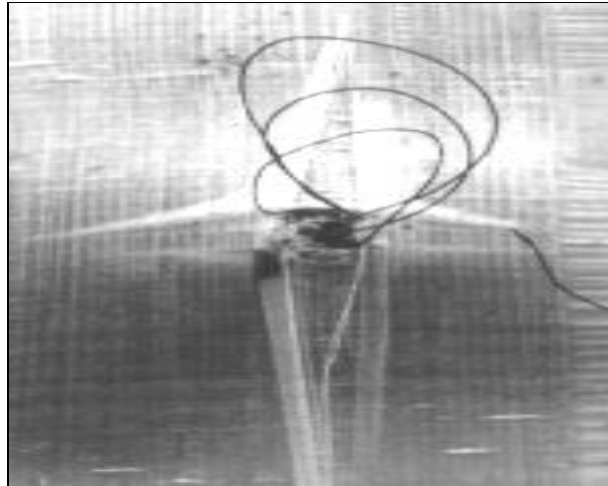


Figure 4.23: Photo of the backface of an impacted ECPE-SMA bi-directional composite specimen demonstrating the characteristic “loop”.

4.8 Summary of V_{50} Ballistic Limit Results

A summary of all the V_{50} ballistic limit test results is shown in Figure 4.24 (next page). From this figure it can be observed that adding uni-directional fibers on the front face or in the middle of the composite does not provide any change in the V_{50} ballistic limit. However, uni-directional SMA fibers placed on the backface of the composite do provide a means to absorb ballistic impact energy, but the addition of a perpendicular SMA ply did not further increase ballistic performance. The addition of ECPE layers on the backface greatly improved the V_{50} ballistic limit in all cases. Furthermore, the SMA fibers performed better when embedded within the strain compatible ECPE.

Also shown in Figure 4.24 is the comparison between the military and logistic regression V_{50} ballistic limit values for all cases. The difference between each method was less than 1%.

4.9 Energy Absorption Comparisons

The increase in energy absorption calculation of the various hybrid configurations with respect to the plain graphite specimens was based on the V_{50} ballistic limit values (Equations 3.3 - 3.4). Since the military and the logistic regression V_{50} ballistic limit velocities have the same values (within 1%), only the military V_{50} ballistic limit velocities were used for the energy calculations. The energy absorption variations for hybrid configurations that displayed more than a 1% increase are shown graphically in Figure 4.25 (next page).

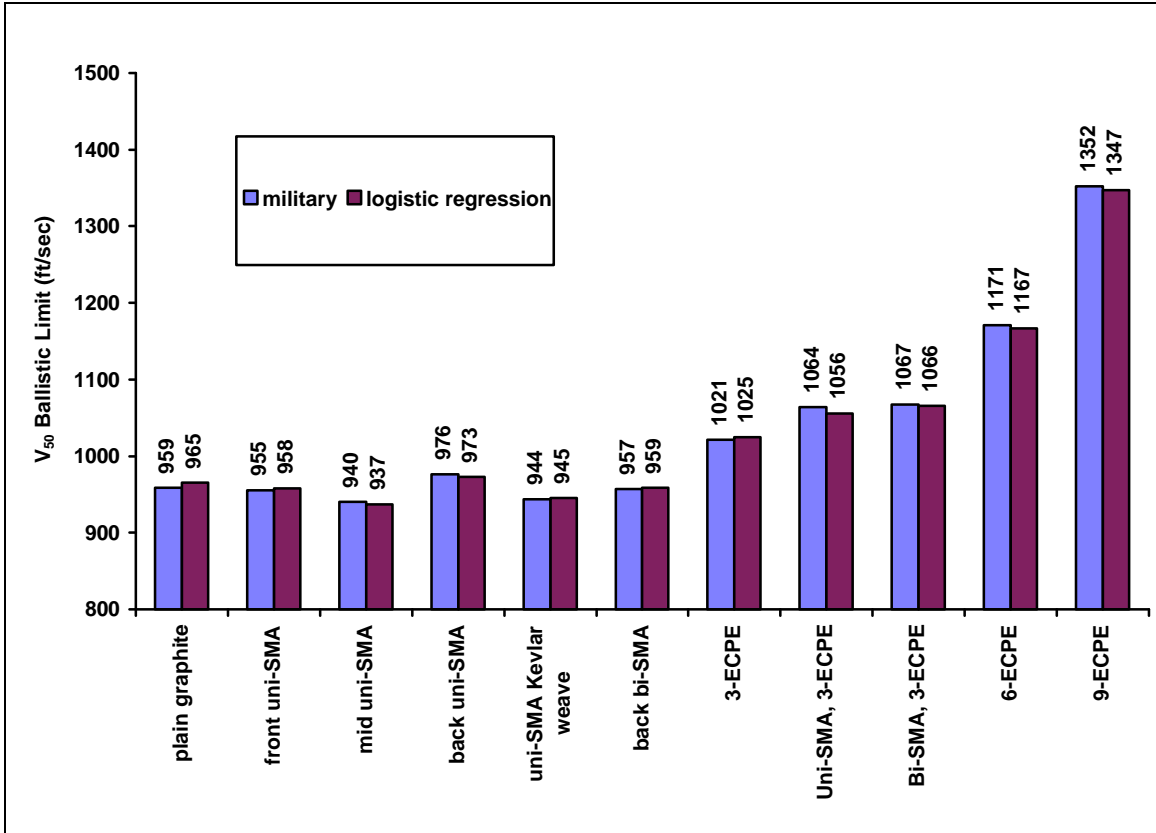


Figure 4.24: Summary of the V_{50} ballistic limit values for each test configuration.

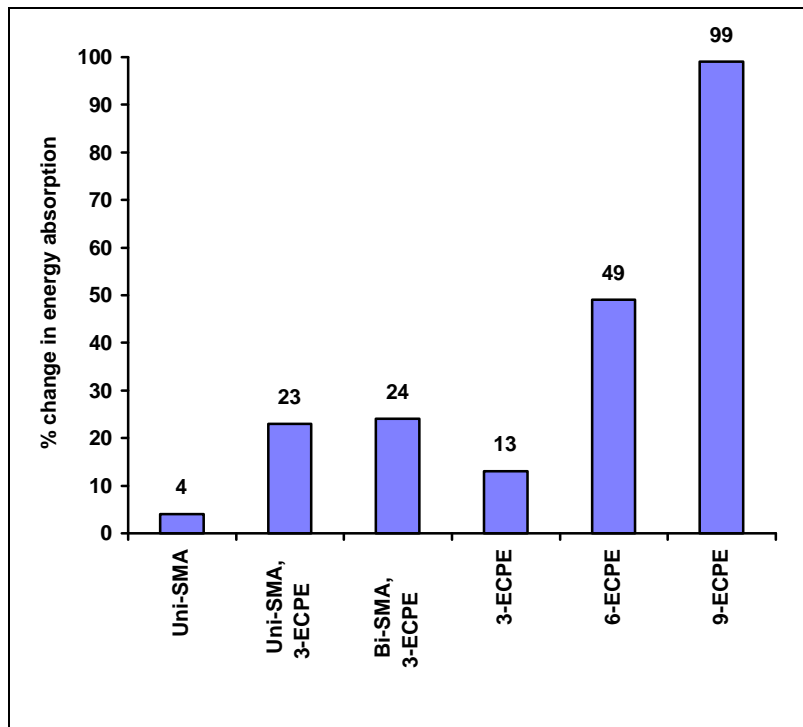


Figure 4.25: Bar graph representing % increases in energy absorption when compared to plain graphite specimens.

The first observation to be made is for the 3, 6, and 9 ECPE layer hybrid configurations: The energy absorption increases exponentially with the addition of ECPE layers. This performance increase contrasts with the use of additional SMA fibers which did not seem to provide an increase in energy absorption (section 4.5). Also, one can notice that the specimens containing three layers of ECPE and uni-directional SMA fibers absorbed about twice that of the specimens containing only three layers of ECPE. With the total weight of one layer of SMA fibers nearly equal to that of three layers of ECPE prepreg (within 10%), as shown in Figure 4.26, the performance of the uni-SMA/3-ECPE hybrid should more appropriately be compared to the 6-ECPE case and the bi-SMA/3-ECPE to the 9-ECPE case when comparing similar weights of hybrid material.

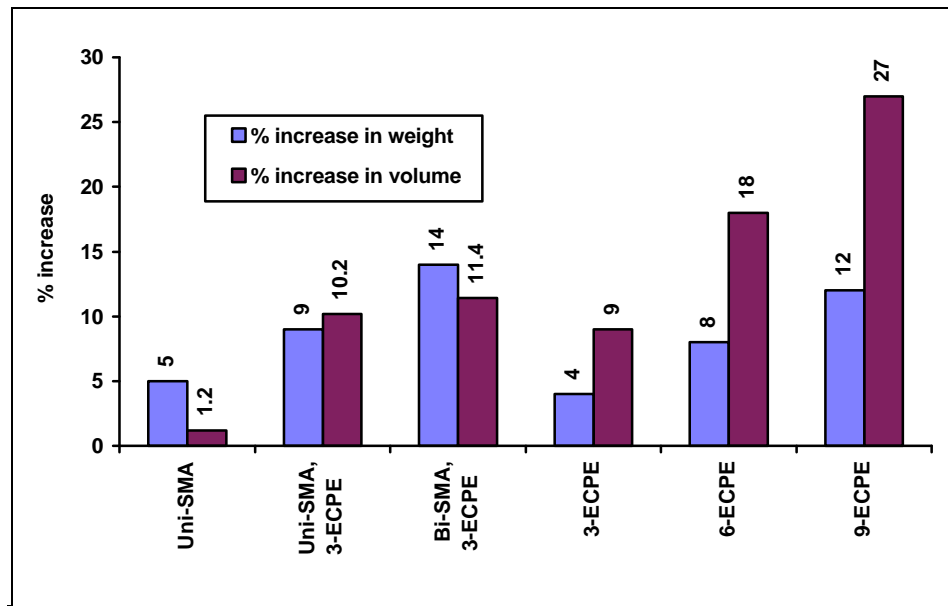


Figure 4.26: Bar graph representing % increases in mass and volume when compared to plain graphite specimens.

Therefore, for a better comparison of results, increases in energy absorption are normalized with respect to weight and volume, as shown in Figure 4.27. Values were calculated from the equations:

$$\% \Delta E_w = \frac{\% \Delta E}{(1 + \% \Delta W)} \quad (4.1)$$

$$\% \Delta E_v = \frac{\% \Delta E}{(1 + \% \Delta V)} \quad (4.2)$$

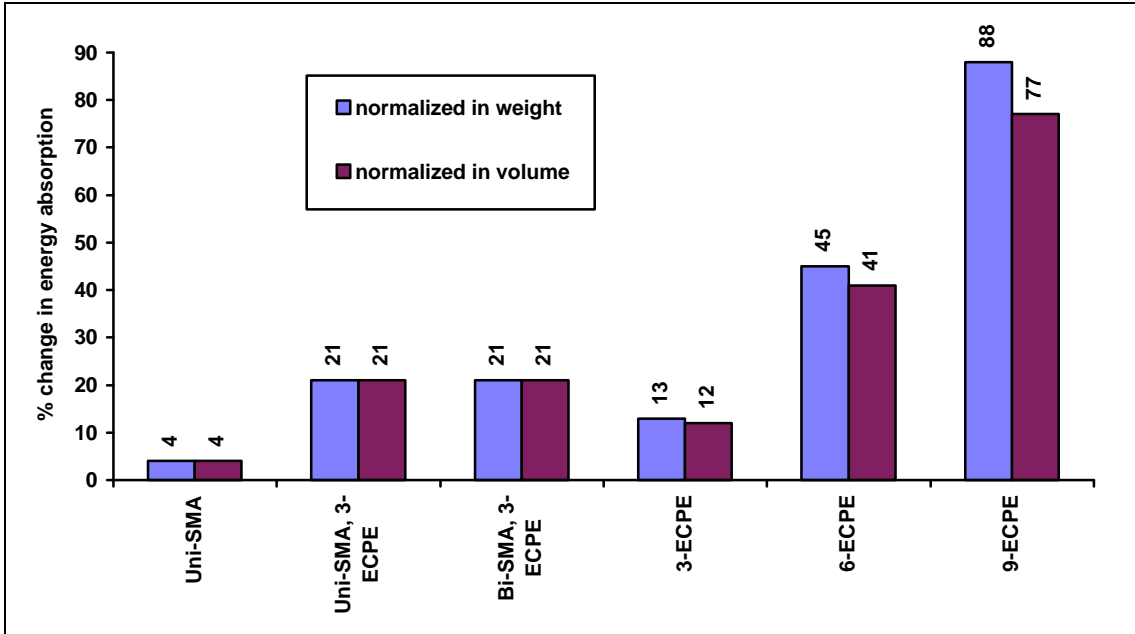


Figure 4.27: Bar graph representing % increases in energy absorption normalized in weight and volume when compared to plain graphite specimens.

Where $\% \Delta E_w$ is the percent change in energy when normalized according to weight, $\% \Delta W$ is the percent change in composite weight, $\% \Delta E_v$ is percent change in energy when normalized according to volume, and $\% \Delta V$ is the percent change in composite volume. When normalized according to weight and volume, the six and nine layer ECPE cases proved to perform significantly better than the uni-SMA, 3-ECPE and bi-SMA, 3-ECPE configurations respectively.

Percent increases in energy absorption with respect to the mass and volume of hybrid components only are shown in Figures 4.28 and 4.29, respectively.

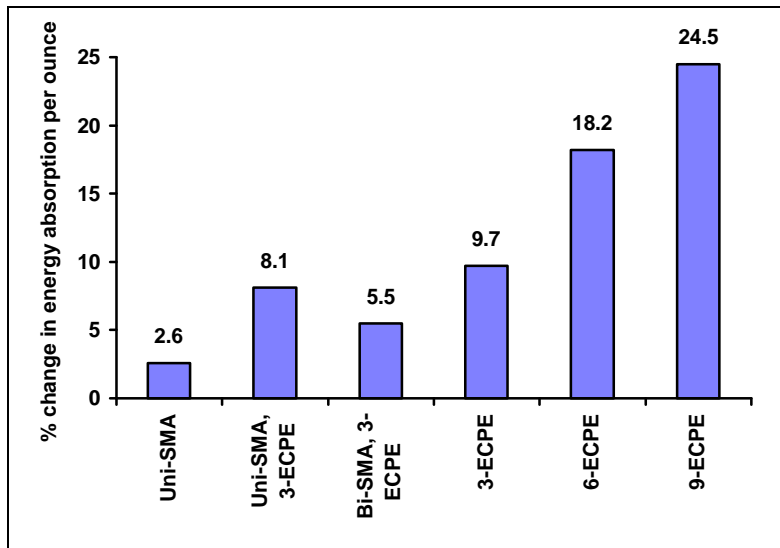


Figure 4.28: Bar graph representing % increases in energy absorption per ounce of hybrid material.

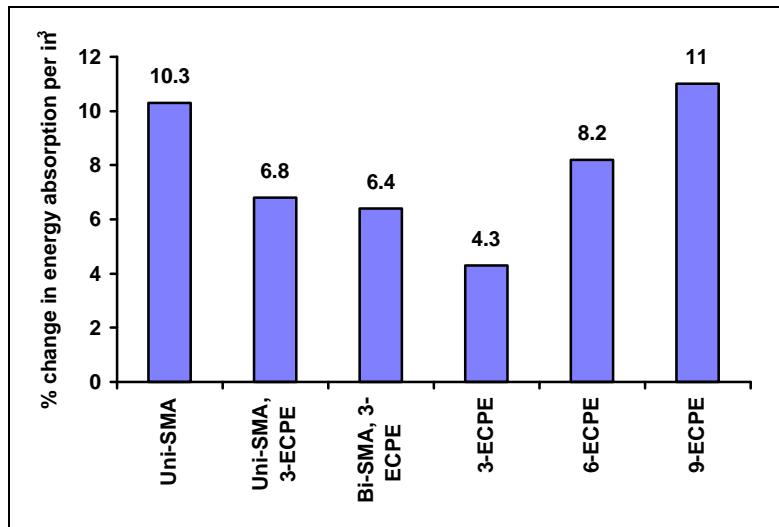


Figure 4.29: Bar graph representing % increases in energy absorption per in³ of hybrid material.

From Figure 4.28 it can be seen that the % increase in energy absorption per ounce of ECPE increases as the mass of material added to the backface is increased. This is also true when considering volume; the % change in energy absorption per in³ of ECPE increases as the volume of material is increased, as shown in Figure 4.29. Also, as shown in Figure 4.29, the % change in energy absorption per volume of SMA added is nearly equal to that of the 9-layer ECPE case. However, this may not be an appropriate comparison since only a 1.2 % volume fraction of SMA was utilized for the uni-SMA case, where a 27 % volume fraction of ECPE was used for the 9-layer ECPE case. As discussed previously, larger volume fractions of SMA did not show any increase in energy absorption (Figure 4.14, Table 4.2).

Chapter 5

Conclusions

The effect of adding small amounts of various high strain hybrid components on the ballistic impact resistance of graphite epoxy composites have been studied in this work. The following conclusions and observations can be made concerning this study.

- Although embedding small amounts of SMA fibers in graphite epoxy composites is very effective at absorbing low velocity impact as demonstrated by the work of Kiesling (1995), it was difficult to utilize the SMA's high strain energy absorption capabilities at ballistic velocities. The SMA fibers would typically be pulled through the graphite without straining to its full potential. It is believed that this is due to high strain rate effects coupled with a strain mismatch between the relatively tough properties of the SMA and the brittle nature of the epoxy resin. Gross fiber pullout and graphite layer breakup resulted.
- It was found that the SMA fibers were more effectively used when embedded in the more ballistically compatible, higher strain, thermoplastic rubber ECPE resin. However, the SMA was still not fully utilized by straining to failure. Instead, the specimen penetration resulted from failure due to SMA single fiber shear pullout.
- Significant increases in energy absorption were found by adding small amounts of ECPE layers to the backface of the composite. A 99% increase in energy absorption was observed with only a 12% increase in total composite mass. In certain design applications, the addition a small amounts of ECPE placed on the backface of the graphite composite would be beneficial. Not only does it provide penetration resistance, but it also allows the designer to reduce the amount of graphite used without compromising the structural strength after impact. This is because a large portion of the impact energy is transferred to the ECPE hybrid component, leaving less energy to go towards damage to the graphite. This is in contrast to an all graphite epoxy panel that would have to be thicker and heavier for the same level of protection where all of the energy imparted by the projectile would go towards degrading the graphite.
- It was found that the backface appeared to be the best location for a high strain hybrid component. On the front and middle locations no increases in energy absorption were observed. It is believed that the SMA fibers were restricted from straining by the surrounding graphite material and were typically cut in shear by the projectile. On the backface, however, it was observed that both the SMA and ECPE fibers could be pulled away from the composite and were free to strain in their axial direction as much as possible.

- The behavior of the deformable projectiles in graphite epoxy panels were much different than the traditional steel projectiles used in most of the literature dealing with ballistic impact resistance. As the projectile penetrated through the composite, its shape and mass was randomly altered. Projectiles penetrating the composite were extremely deformed with many sharp edges and portions of the projectile often being left within the composite.
- Less than a 1% difference existed between V_{50} ballistic limit velocities calculated from the military standard (MIL-STD-663E) and logistic regression analysis. This indicates that both methods are suitable.

Chapter 6

Recommendations

It has been shown that the implementation of a high strain material on the backface of a structural composite element is an effective method for improving the absorption of the impact energy of a projectile traveling at ballistic velocities. In order to further substantiate this conclusion, the following recommendations are given.

- The SMA fibers ability to absorb energy under ballistic impact has yet to be established since the SMA was pulled out of the composite before being allowed to strain to its full potential. Therefore different fabrication methods should be explored. In a design application, the SMA fibers are likely to be greater in length, which could inhibit the SMA fiber from being pulled out all the way to its ends. This would allow the SMA fibers to be strained to its full potential. In order to simulate this type of situation, further tests could be performed where the SMA fibers extend beyond the specimen edges and are rigidly anchored.
- In this study, creating an SMA weave component was attempted. However, because of the superelastic nature of the SMA and its inability to crimp, it was difficult to get a tight fiber mesh. It would be beneficial to explore other weaving methods and configurations that do not require the material to be crimped. One type of approach would be to create a weave similar to a chain link fence, as shown in Figure 6.1.

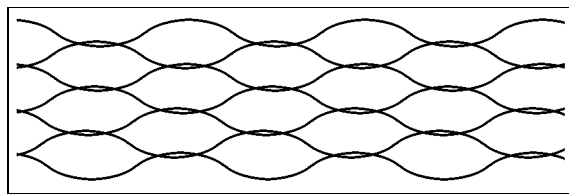


Figure 6.1: Drawing of suggested SMA weave pattern.

- Another area of study that merits further investigation is the effect of different sizes and shapes of SMA wire. It is expected that improvements in energy absorption would be obtained by using a smaller fiber diameter with the same volume fraction of SMA. Hence, although the strain mismatch still exists, since the total bonding area of the SMA fibers would be increased, it would require more energy to break that bond. Thus, it is expected that an increase in energy absorption would be observed.

- The use of non-deformable projectiles for testing of the components used in this study warrants investigation. This would prevent the creation of sharp edges and projectile breakup. It is expected that, although penetration values may be different, the principal damage mechanisms will remain the same.
- In this study, it has been observed that a portion of the energy transferred from the projectile to the hybrid composite is absorbed by the high strain ECPE hybrid component, thus reducing the amount of energy going towards damage to the graphite epoxy component. However, this observation still needs to be proven with post impact composite strength tests.
- The ECPE hybrid components were not tested on the front and middle faces of the composite based on observations made from the SMA tests. It was presumed that the ECPE would behave in a manner similar to the SMA; which remains to be proven.
- In this study, it was found that the military approach and the logistic regression analysis approach to determine the V_{50} ballistic limit provided similar results. However, further tests incorporating a larger number of data points are needed to validate this observation.
- Finally, it would be interesting to test metallic fibers, such as aluminum and high strength steel to determine the effect of the SMA's stress induced martensitic phase transformation as an energy absorption mechanism.

References

Adams, D.F., and Miller, A.K., 1975, "An Analysis of the Impact Behavior of Hybrid Composite Materials", *Materials Science and Engineering*, Vol. 19 (1975), pp. 245-260.

Azzi, B., Bless, S., and Brar, N.S., 1991, "Force Measurements Projectiles Penetrating Fiber Reinforced Composite Targets", 23rd International SAMPE Technical Conference, October 21-24, 1991, pp. 616-623.

Bascom, W.D., Gweon, S.Y., and Grande, D., 1993, "Multiphase Matrix Polymers for Carbon-Fiber Composites", *Advances in Chemistry*, No. 208, pp. 519-537.

Beaumont, P.W.R., Riewald, P.G., and Zweben, C., 1974, "Methods for improving the impact resistance of Composite Materials", *Foreign Object Impact Damage to Composites*, ASTM STP 568, pp. 134-158

Bhatnagar, A., Lin, L.C., Lang, D.C., and Chang, H. W., 1989, "Comparison of Ballistic Performance of Composites", 34th international SAMPE Symposium, May 8-11, 1989, pp. 1529-1537.

Bless, S.J., and Hartman, D.r., 1989, "Ballistic Penetration of S-2 Glass® Laminates", 21st International SAMPE Technical Conference, September 25-28, 1989, Vol. 21, pp. 852-866.

Bradshaw, F.J., Dorey, G., and Sidney, G.R., 1972, "Impact Resistance of Carbon Reinforced Plastics", MOD, RAETR 72240.

Cantwell W.J., and Morton, J., 1989(a), "Geometrical Effects in the Low Velocity Response of CFRP", *Composites Structures*, Vol. 12, pp. 39-59.

Cantwell, W.J., and Morton, J., 1989(b), "Comparison of the low and high velocity impact response of CFRP", *Composites*, Vol. 20, No. 6, pp. 545-551.

Cantwell, W.J., and Morton, J., 1989(c), "The Influence of Varying Projectile Mass on the Impact Response of CFRP", *Composite Structures*, vol. 13, pp. 101-114.

Cantwell, W.J., and Morton, J., 1990(a), "Impact Perforation of Carbon Fibre Reinforced Plastic", *Composites Science and Technology*, 38(1990), pp. 119-141.

Cantwell, W.J., and Morton, J., 1990(b), "An Assessment of the Residual Strength of an Impact-Damaged Carbon Fibre Reinforced Epoxy", *Composite Structures*, Vol. 14, pp. 303-317.

Cantwell, W.J., and Morton, J., 1991, "The impact resistance of composite materials - a review.", *Composites*, Vol. 22, No. 5, pp. 347-362.

Cantwell, W.J., Curtis, P.T. & Mortin, J., 1983, "Post impact fatigue performance of carbon fiber laminates with non-woven and mixed-woven layers.", *Composites*, Vol. 14, No. 3, pp. 301-305.

Cantwell, W.J., Curtis, P.T., and Morton J., 1986, "An assessment of the impact performance of CFRP reinforced with high-strain carbon fibers.", *Composite Science and Technology*, Vol. 25, pp. 133-148.

Callister, W.D., 1994, Material Science and Engineering, 4th ed., John Wiley & Sons, Inc.

Chamis, C.C., Hanson, M.P., and Serafini, T.T., 1972, "Impact Resistance of Unidirectional Fiber Composites", *Composite Materials: Testing and Design (Second Conference)*, ASTM STP 497, pp. 311-323.

Chan, W.S., Rogers, C., and Aker, S., 1986, "Improvement of Edge Delamination Strength of Composite Laminates Using Adhesive Layers", *Composite Materials Testing and Design*, ASTM STP 893, pp. 266-285.

Choi, H.Y. and Chang, F., 1991, "A New Approach Toward Understanding Damage Mechanisms and Mechanics of Laminated Composites Due to Low-Velocity Impact", *Journal of Composite Materials*, Vol. 25, pp. 992-1038.

Choi, H.Y., 1991, "Damage in Graphite/Epoxy Laminated Composites Resulting From Low Velocity Impact", AIAA-91-1081-CP, pp. 1153-1161.

Choi, H.Y., Wang, H.S., and Chang, F., 1992, "Effect of Laminate Configuration and Impactor's Mass on the Initial Impact Damage of Graphite/Epoxy Composite Plates Due to Line-Loading Impact", *Journal of Composite Materials*, Vol. 26, No. 6, pp. 804-827.

Cristescu, N., Malvern, L.E., and Sierakowski, R.L., 1975, "Failure Mechanisms in Composite Plates Impacted by Blunt-Ended Penetrators," *Foreign Object Impact Damage to Composites*, ASTM STP 568, pp. 159-172.

Cordova, D.S., and Bhatnager, A., "High Performance Hybrid Reinforced Fiber Composites: Optimizing Properties with PE Fibers", *Tech. Pub. of Allied Fibers Tech. Center, Petersburg, Virginia*, 1987. Also at 32nd SAMPE Conf. and Exhibits, Anaheim, California, 4-9 April 1987.

Cuniff, P.M., 1992, "An Analysis of the System Effects in Woven Fabrics Under Ballistic Impact", *Textile Research Journal*, Vol. 62, No. 9, pp. 495-509.

Cuniff, P.M., Song, J.W., and Ward, J.E., 1989, "Investigation of High Performance Fibers for Ballistic Impact Resistance Potential", 21st International SAMPE Technical Conference, September 25-28, 1989, pp. 840-847.

Curtis, P.T., 1984, "An Initial Evaluation of a High-Strain Carbon Fiber Reinforced Epoxy", Royal Aircraft Establishment, TR 84004.

Deluca, J.L., and Petrie, S.P., 1990, "Evaluation of Lightweight Material Concepts for Aircraft Turbine Engine Rotor Protection", 22nd International SAMPE Technical Conference, Nov. 6-8, 1990, Vol. 22, pp. 319-333.

Dikshit, S.N., and Sundararajan, G., 1992, "Effect of Clamping Rigidity of the Armour on Ballistic Performance", Defense Science Journal, Vol. 42, No. 2, pp. 117-120.

Dikshit, S.N., Kutumbarao, V.V., and Sundararajan, G., 1995, "The Influence of Plate Hardness on the Ballistic Penetration of Thick Steel Plates", International Journal of Impact Engineering, Vol. 16, No. 2, pp. 293-320.

Dorey, G., 1974, "Fracture Behavior and Residual Strength of Carbon Fiber Composites Subjected to Impact Loads," AGARD CP163, Paper B2, Advisory Group for Aerospace Research and Development, pp. 8-1 through 8-12.

Dorey, G., "Impact and crashworthiness of composite structures.", Structural Impact and Crashworthiness", Vol. 1, ed. G. A. O. Davies, Elsevier Applied Science Publishers, London, 1984.

Dorey, G., Sidney, G.R., and Huchings, J., 1978, Impact properties of carbon fiber/Kevlar 49 fiber hybrid composites", Composites, January, 1978, pp. 25-32.

Gillespie Jr, J.W., Carlson, L.A., and Smiley, A.J., 1987, "Rate dependent Mode I interlaminar crack growth mechanisms in graphite/epoxy and graphite/PEEK", Composites Science and Technology, Vol. 28, pp. 1-15.

Gupta, N.K., and Madhu, V., 1992, "Normal and Oblique Impact of a Kinetic Energy Projectile on Mild Steel Plates", International Journal of Impact Engineering, Vol. 12, No. 3, pp. 333-343.

Harris, B., and Bunsell, A.R., 1975, "Impact properties of glass fiber/carbon fiber hybrid composites", Composites, Sept. 1975, pp. 197-201.

Heatherington, J.G., 1992, "The Optimization of Two Component Composite Armors", International Journal of Impact Engineering, Vol. 12, No. 3, pp. 409-414.

Heatherington, J.G., and Rajagopalan, B.P., 1991, "An Investigation Into the Energy Absorbed During Ballistic Perforation of Composite Armors", *International Journal of Impact Engineering*, Vol. 11, No. 1, pp. 33-40.

Hedrick, J.C., Niranjana, M.P., and McGrath, J.E., 1993, "Toughening of Epoxy Resin Networks with Functionalized Engineering Thermoplastics", *Advances in Chemistry*, No. 208, pp. 293-304.

Hoisington, M.A., and Seferis, J.C., 1993, "Model Multi-layer Toughened Thermosetting Advanced Composites", *Advances in Chemistry*, No. 208, pp. 505-518.

Hsieh, C.Y., Mount, A., Jang, B.Z., and Zee, R.H., 1990, "Response of Polymer Composites to High and Low Velocity Impact", 22nd International SAMPE Technical Conference, Nov. 6-8, 1990, Vol. 22, pp. 14-27.

Huang, Y., Kinloch, A.J., Bertsch, R.J., and Siebert, A.R., 1993, "Particle-Matrix Interfacial Bonding: Effect on the Fracture Properties of Rubber-Modified Epoxy Polymers", *Advances in Chemistry*, No. 208, pp. 189-210.

Hunston, D.L., et al., 1987, "Matrix resin effects in composite delamination: mode I fracture aspects", *Toughened Composites*, ASTM STP 937, pp. 74-79.

Husman, G.E., Whitney, J.M., and Halpin, J.C., 1975, "Residual Strength Characterization of Laminated Composites Subjected to Impact Loading", *Foreign Object Impact Damage to Composites*, ASTM STP 568, pp. 92-113.

Jang, B.Z., and Chung, W.C., 1986, "Structure-property relationships in three-dimensionally reinforced fibrous composites", *Advanced Composites: Latest Developments*, ASM International, pp. 183-192.

Jang, B.Z., Chen, L.C., Wang, C.Z., Lin, H.T., and Zee, R. H., 1989, "Impact Resistance and Energy Absorption Mechanisms in Hybrid Composites", *Composites Science and Technology*, Vol. 34, pp. 305-335.

Jenq, S.T., Jing, H.S., and Chung, C., 1994, "Predicting the Ballistic Limit for Plain Woven Glass/Epoxy Composite Laminate", *International Journal of Impact Engineering*, Vol. 15, No. 4, pp. 451-464.

Jenq, S.T., Wang, S.B., and Sheu, L.T., 1992, "A Model for Predicting the Residual Strength of GFRP Laminates Subject to Ballistic Impact", *Journal of Reinforced Plastics and Composites*, Vol. 11, pp. 1127-1141.

Kang, T.J., and Lee, S.H., 1994, "Effect of Stitching on the mechanical and Impact Properties of Woven Laminate Composite", *Journal of Composite Materials*, Vol. 28, No. 16, pp. 1574-1587.

Kiesling, T.C., 1995, "Impact Failure Modes of Graphite Epoxy Composites with Embedded Superelastic Nitinol", Masters Thesis, Mechanical Engineering Dept., VPI&SU, Blacksburg, Virginia.

Kiesling, T.C., Chaudhry, Z., Paine, J.S.N., and Rogers, C.A., 1996, "Impact Failure Modes of Thin Graphite Epoxy Composites Embedded with Superelastic Nitinol", Proceedings, 37th AIAA/ASME/ASCE/AHS/ASC Structures, Structural Dynamics, and Materials Conference, Salt Lake City, Utah, 15-17 April 1996, pp. 1448-1457.

Lagace, P.A. and Wolf, E., 1993, "Impact Damage Resistance of Several Laminated Material Systems", Proceedings of the Structural Dynamics and Materials Conference, AIAA-93-1524-CP, AIAA, pp. 1863-1872.

Lee, B.L., Song, J. W., and Ward, J.E., 1994, "Failure of Spectra® Polyethylene Fiber-Reinforced Composites Under Ballistic Impact Loading", Journal of Composite Materials, Vol. 28, No. 13, pp. 1202-1226.

Lin, L.C., Bhatnager, A., and Chang, H.W., 1990, "Ballistic Energy Absorption of Composites", 22nd International SAMPE Technical Conference, pp. 1-13.

Lin, L.C., and Bhatnager, A., 1992, "Ballistic Energy Absorption of Composites - III", 24th International SAMPE Technical Conference, Vol. 24, pp. 291-306.

Maiden, J.R., and Ebersole, T.S., 1991, "Development of Composite Structures With Enhanced Damage Tolerance", 23 International SAMPE Technical Conference, October 21-24, 1991, Vol. 23, pp. 855-869.

Manders, P.W., and Bader, M.G., "The strength of hybrid glass/carbon fiber composites. Part I. Failure strain enhancement and failure mode.", Journal of Material Science, Vol. 16, pp. 2233-2245.

Marom, G, Drukker, E., Weinberg, A., and Banbaji, J., 1986, "Impact Behavior of carbon/Kevlar hybrid composites", Composites, Vol. 17, No. 2, pp. 150-153.

Novak, R.C., and DeCrescente, M.A., 1972, "Impact Behavior of Unidirectional Resin Matrix Composites Tested in the Fiber Direction", Composite Materials (Second Conference), ASTM STP 497, pp. 311-323.

Opplinger, D.W., and Slepetz, J.M., 1975, "Impact Damage Tolerance of Graphite/Epoxy Sandwich Panels", Foreign Object Impact Damage to Composites, ASTM STP 568, pp. 30-48.

Pageau, G, Vaziri, R., and Poursartip, A., 1991, "An Evaluation of Metal Matrix Composites as Ballistic Protection Materials", 22nd International SAMPE Technical Conference, October 21-24, 1991, pp. 639-650.

Paine, J.S.N., 1994, "Multi-Functional SMA Hybrid Composite Materials and Their Applications", Ph.D. Dissertation, Mechanical Engineering Dept., VPI&SU, Blacksburg, Virginia.

Paine, J.S.N., and Rogers, C.A., 1994, "The response of SMA Hybrid Composite Materials to Low Velocity Impact", Journal of Intelligent Material Systems and Structures, Vol. 5-July 1994, pp. 530-535.

Paine, J.S.N., and Rogers, C.A., 1995, "Observations of the Drop-weight Impact Response of Composites with Surface Bonded Nitinol Layers", Durability and Damage Tolerance of Composites Symposium, 1995 ASME IMEC&E, San Francisco, CA, Nov. 12-18, 1995.

Pavithran, C., Mukherjee, P.S., Brahmakumar, M., and Damodaran, A.D., 1991, "Impact properties of sisal-glass hybrid laminates", Journal of Material Science, Vol. 26, pp. 455-459.

Peijs, A.A.J.M., and Venderbosch, R.W., 1991, "Hybrid composites based on polyethylene and carbon fibers Part IV Influence of hybrid design on impact strength", Journal of Materials Science and Letters, Vol. 10, pp. 1122-1124.

Poursartip, A., Riahi, G., Teghtsoonian, E., Chinatambi, N., and Mulford, N., 1987, "Mechanical properties of PE fiber/carbon fiber hybrid laminates", ICCM-VI and ECCM-II, Vol. 1, Elsevier Applied Science, pp. 209-220.

Rechak, S., and Sun, C.T., 1990, "Optimal Use of Adhesive Layers in Reducing Impact Damage in Composite Laminates", Journal of Reinforced Plastics and Composites, Vol. 9, pp. 569-582.

Savrun, E., Tan, C. Y., and Robinson, J., 1991, "Ballistic Performance of Ceramic Faced Armors," 23d International SAMPE Technical Conference, October 21-24, Vol. 23, pp. 661-668.

Schonberg, W.P., and Yang, F., 1993, "Response of Space Structures to Orbital Debris Particle Impact", Int. J. Impact Eng., Vol. 14, pp. 647-658.

Schwinghamer, R.J., 1993, "Shield Design for Protection against Hypervelocity Particles", NASA Tech Briefs, December 1993, pp. 76-77.

Scott, R.F., Lee, S., Poon, C., and Gaudert, P.C., 1991, "Impact and Compression Response of Composite Materials Containing Fortifiers", *Polymer Engineering and Science*, Vol. 31, No., 18, pp. 1310-1315.

Sloan, F., and Nguyen, H., 1995, "Mechanical Characterization of Extended-Chain Polyethylene (ECO) Fiber-Reinforced Composites" *Journal of Composite Materials*", Vol. 29, No. 16, pp. 2092-2107.

Su, K.B., 1989, "Delamination Resistance of Stitched Thermoplastic Matrix Composite Laminates", *Advances in Thermoplastic Matrix Composite Materials*, ASTM STP 1044, pp. 279-300.

Suarez, J.A., and Whiteside, J.B., 1975, "Comparison of Residual Strength of Composite and Metal Structures After Ballistic Damage", *Foreign Object Impact Damage to Composites*, ASTM STP 568, pp. 72-91.

Sun, C.T., and Rechak, S., 1988, "Effect of Adhesive Layers on Impact Damage in Composite Laminates", *Composite Materials Testing and Design*, ASTM STP 972, pp. 97-123.

Walters, W., and Scott, B.R., 1990, "High Velocity Penetration of a Kevlar® Reinforced Laminate", *22nd International SAMPE Technical Conference*, November 6-8, 1990, pp. 1078-1091.

Wang, C.J., and Jang, B.Z., 1991, "Deformation and Fracture Mechanisms of Advanced Polymer Composites Under Impact Loading", *Journal of Thermoplastic Composite Materials*, Vol. 4, pp. 140-172.

Wang, H., and Vu-Khanh, 1991, "Impact-Induced Delamination in [0₅,90₅,0₅] Carbon Fiber/Polyetheretherketone Composite Laminates", *Polymer Engineering and Science*, Vol. 31, No. 18, pp. 1301-1309.

Wardle, M.W., 1982, "Impact Damage Tolerance of Composites Reinforced with Kevlar® Aramid Fibers", *Progress in Science and Engineering of Composites*", Vol. 1, pp. 837-844.

Williams, J.G., and Rhodes, M.D., 1982, "Effects of resins on impact damage tolerance of graphite/epoxy laminates. ASTM STP 787, 450.

Wright, S.C., Fleck, N.A., and Stronge, W.J., 1993, "Ballistic Impact of Polycarbonate - An Experimental Investigation", *International Journal of Impact Engineering*, Vol. 13, No. 1, pp. 1-20.

Zee, R.H., Wang, C.J., Mount, A., Jang, B.J., and Hsieh, C.Y., 1991, "Ballistic Response of Polymer Composites", *Polymer Composites*, Vol. 12, No. 3, pp. 196-202.

Zhu, G., Goldsmith, W., and Dharan, C.K.H., 1992, "Penetration of Laminated Kevlar by Projectiles - I. Experimental Investigation", *International Journal of Solids and Structures*, Vol. 29, No. 4, pp. 399-420.

Vita

Roger Lee Ellis was born in Flagstaff, Arizona on February 19, 1970. He grew up in Colorado Springs, Colorado where he graduated from Doherty High School in 1988. After high school, he attended Ricks College in Rexburg, Idaho for one year. Then for two years he interrupted his undergraduate education to serve in Ohio as a representative of the Church of Jesus Christ of Later-Day Saints. He then returned to Ricks College in 1991. After receiving his Associates degree in Mechanical Engineering in 1992, he transferred to Utah State University. While at Utah State, he met and married the love of his life, Andrea. In 1995, he received his Bachelor of Science degree in Mechanical Engineering. He is currently working on his Master of Science degree at Virginia Polytechnic Institute and State University.